Disease Markers 19 (2004) 49–68
IOS Press

In vivo measurement of phosphorous markers of disease

Fernando Arias-Mendoza[a,*] and Truman R. Brown[a,b]
[a]*Hatch Center for MR Research, Department of Radiology, Columbia University, New York, NY, 10032, USA*
[b]*Department of Biomedical Engineering, Columbia University, New York, NY, 10032, USA*

Abstract. Phosphorus Magnetic Resonance Spectroscopy (^{31}P-MRS) has been utilized to study energy, carbohydrate, and phospholipid metabolism *in vitro* and *in vivo* in live tissues non-invasively. Despite its lack of sensitivity, its application has extended to *in situ* human tissues and organs since proper signal localization was devised. Follow-up of phosphocreatine in neuromuscular diseases and schizophrenia and follow-up of phospholipid-related molecules in tumors are described here to demonstrate the value of ^{31}P-MRS as an imaging technique to determine *in vivo* markers of disease and in the diagnosis, prognosis, and follow-up of human diseases.

Keywords: ^{31}P MR spectroscopy, chemical shift imaging, *in vivo* metabolism, neuromuscular disease, mitochondrial cytopathy, schizophrenia, non-Hodgkin's lymphoma, chronic lymphocytic leukemia

Abbreviations: NMR, nuclear magnetic resonance; MRI, magnetic resonance imaging; MRS, magnetic resonance spectroscopy; CSI, chemical shift imaging; Etn-P phosphoethanolamine; Cho-P, phosphocholine; Pi, inorganic phosphate; Gro-P-Etn, glycero-phosphoethanolamine; Gro-P-Cho, glycero-phosphocholine; NTP, nucleotide triphosphates; NDP, nucleotide diphosphates; UDP, uridine diphosphate; PCr, phosphocreatine; PL, phospholipids; SNR, signal to noise ratio; NOE, nuclear Overhausser enhancement; RF, radiofrequency; ND, neuromuscular diseases; MC, mitochondrial cytopathy; ATP, adenosine triphosphate; CoQ_{10}, Coenzyme Q_{10}; BN, below-normal; NN near-normal (memory scores); NHL, non-Hodgkin's lymphoma; IPI, international prognostic index; TTF, time to treatment failure; CCL, chronic lymphocytic leukemia

1. Historical background

In the past three decades, nuclear magnetic resonance (NMR), an analytical technique initially utilized to elucidate the structure and composition of molecules, has become a methodology that allows the study of live samples. The basic principle of NMR is that nuclei with a nuclear spin in a magnetic field show resonances at various frequencies proportional to the magnetic field. The strengths of these signals are proportional to the amount of their originating nuclei, and their frequencies depend on the molecule in which they are located. Many of these signals can be observed from living systems because the microenvironment inside cells and tissues resembles free solutions on a microscopic scale. Initial observations of living systems consisted of cells and isolated organs in high field, small bore magnets [1, 2]. With the development of magnetic resonance imaging (MRI) technology, large magnets at intermediate magnetic fields have become available, and these studies have been extended to humans. Parallelling the developments in magnetic technology were similar improvements in spectral localization techniques. Localization began with MRI, which primarily uses the strong ^{1}H signal of water in biological tissues and occasionally the ^{1}H signal from the methylenes of fatty acids. This development led to localized *in vivo* magnetic resonance spectroscopy (MRS) a few years latter with the development of single- and double-volume localization techniques. The early work was well re-

*Corresponding author: Fernando Arias-Mendoza, MD, PhD, Hatch Center for MR Research, Department of Radiology, Columbia University, 710 W. 168th Street, Neurological Institute Basement, New York, NY 10032, USA. Tel.: +1 212 305 1169; Fax: +1 212 314 3557; E-mail: fa2003@columbia.edu.

ISSN 0278-0240/02/$8.00

viewed by Bottomley and colleagues [2]. More complex multiple-volume methodology for spectroscopy, chemical shift imaging (CSI), capable of isolating spectra in three dimensions, was developed by Brown and colleagues in 1983 [3]. Recently, even higher magnetic fields (4–7 T) have become available, which suggests substantial improvement in spectral and image resolution *in vivo* in the future.

The most extensively used nuclei in the study of live samples by MRS have been phosphorus-31 (^{31}P), carbon-13 (^{13}C), and hydrogen-1 (^{1}H). In every case, the nuclear spins that can be observed are those in relatively small molecules (<5–10 kD) that can tumble in solution sufficiently quickly to produce a sharp resonance. The natural abundance of ^{31}P is 100% of the available pool of phosphorus molecules, but its spectroscopic sensitivity is lower than ^{1}H, which allows visualization of phosphorus-containing molecules with a concentration in the millimolar range. However, the molecules in living matter that can be visualized by ^{31}P MRS are very important because they are linked to bioenergetics, the metabolism of carbohydrates, and the turnover of phospholipids and membranes. Note that, though phospholipids, membranes, polynucleotide molecules (i.e., DNA, RNA), and even bone constituents have a large amount of phosphorus, they are not observed as sharp lines becaus they are not able to tumble rapidly enough. On the other hand, ^{13}C has a natural abundance of only 1.1% and its sensitivity is slightly lower than ^{31}P. The natural abundance signals of ^{13}C in living matter show only storage molecules with repetitive units (i.e., glycogen and fatty acids). However, experiments with ^{13}C-enriched molecules have demonstrated intermediates and end products of metabolic pathways from which many inferences about metabolic regulation of such pathways can be drawn. Finally, ^{1}H is the most sensitive of the resonant nuclei. Its natural abundance is almost 100%, and almost all biological molecules have hydrogen. The high sensitivity and abundance issues could allow visualizing many biologically important molecules but a smaller range of resonant frequencies makes it harder to distinguish signals from different compounds. The very large signals from hydrogen in water and lipids in living samples that obscure visualization of other ^{1}H signals from metabolites of much lower concentration are another drawback. Nevertheless, the fact that MRI is based on ^{1}H signals from water and lipids has made the clinical imagers accessible to collect ^{1}H-MRS. This is why proton spectroscopy has been more available for *in vivo* applications in humans. Although the nuclei listed above (i.e., ^{31}P, ^{13}C, ^{1}H) have been the dominant ones applied to studies *in vivo*, other nuclei also have demonstrated potential to be used *in vivo* (i.e., nitrogen-15, fluorine-19, and sodium-23) [4]. In this review, we focus on the applications and advancements of ^{31}P MR spectroscopy in the study of biological samples *in vivo*, with special regard for the possible role of this technique in identifying markers of disease in humans.

2. Spectral information contained in phosphorus MRS of live samples

Phosphorus MRS (^{31}P-MRS) initially was believed to have the best potential for use in biological research due to the nature of the biological information obtained. An example of this is shown in the spectrum at the bottom of Fig. 1, which is an ^{1}H-decoupled ^{31}P MR spectrum of a perchloric acid extract of human lymphocytes from a normal volunteer acquired at 9.4 T (see figure caption for acquisition parameters) [5]. Four expanded regions of the same spectral area are shown in the lower portions of insets A–D. This well-resolved spectrum is due to the higher magnetic field strength and the highly homogeneous aqueous solution of the extract. In the lower spectrum of the main panel of Fig. 1, the signals of the phospholipid-related phosphomonoesters, phosphoethanolamine (Etn-P) and phosphocholine (Cho-P), are shown in extracted normal lymphocytes. The larger signal downfield from Etn-P ($\sim$3.0 ppm) in the spectrum corresponds to inorganic phosphate (Pi). The Pi concentration in this particular spectrum is biologically meaningless due to contamination by the phosphate-based buffers utilized in the extraction procedures [5]. The smaller signals between Cho-P and Pi present in the spectrum have not been identified. Inset A shows the region where phosphodiesters (mainly glycerophosphoethanolamine [Gro-P-Etn] and glycerophosphocholine [Gro-P-Cho]) resonate. Inset B shows the resonant area of the terminal phosphates of nucleotide polyphosphates. In living tissues, these signals mainly are the resonances of the γ phosphate of nucleotide triphosphates (γ-NTP) and the ß phosphate of nucleotide diphosphates (ß-NDP). These signals are split in two peaks (doublets) due to their interaction with the neighboring phosphorus in the anhydride chain. Inset C in Fig. 1 shows the doublet signals of the initial phosphates (a) of the anhydride chain in NDP and NTP and the phosphates of several diphosphoadsesters (i.e., UDP-sugars, nicotine adenine dinucleotide) not fully identified (region X).

Finally, inset D shows the triplet signal of the middle phosphate of the anhydride chain in NTP (ß-NTP). In contrast, spectrum A of Fig. 2 (from [6]) shows the ^{31}P MR signals from a whole human head *in vivo* at 1.5 T (see figure caption for acquisition parameters). As expected, the more inhomogeneous conditions of study and the lower magnetic field strength resulted in lower spectral resolution. Although in different ratios, the signals in Fig. 1 also are present in Fig. 2. Conversely, spectrum A in Fig. 2 shows signals that are not present in Fig. 1. Phosphocreatine (PCr) is selectively present, depending on the particular tissues involved (i.e., brain, muscle, and heart), but is not present in lymphocytes. The broad phospholipid (PL) signal under the sharp signals from spectrum A in Fig. 2, although present in variable concentrations in all tissues, is lost in an acid extract such as the one used to obtain the spectra shown in Fig. 1. Furthermore, spectrum B in Fig. 2, acquired from the same human head, does not show the PL signal because an off-center Gaussian pulse as described elsewhere [6] was used to saturate this broad signal, which in turn has improved the baseline of the sharp signals.

The signals from the normal tissue spectra shown in Figs 1 and 2 exemplify the information that ^{31}P MR spectroscopy can provide: Cho-P, Etn-P, Gro-P-Cho, Gro-P-Etn, and PL are metabolites in the phospholipid and membrane turnover; UDP-sugars are intermediates in the carbohydrate metabolism; and NTP, NDP, Pi, and PCr participate in bioenergetics. Furthermore, due to the interaction of Pi with free protons (H^+) and NTP with H+ and magnesium (Mg^{+2}) and the near-equilibrium of these interactions in biological tissues, the Pi and NTP signals modify their resonant frequencies according to the concentrations of H^+ (pH) and Mg^{2+} *in vivo* [7,8]. However, these interactions are lost when a tissue is extracted to obtain an aqueous solution.

3. Recent technical advances for human applications of *in vivo* ^{31}P-MRS

3.1. Three-dimensional spectroscopic localization

Since its original publication in 1982 [3], chemical shift imaging (CSI) has been the technique of choice to carry out multivolume MRS localization irrespective of the nucleus studied. Since then, more than 250 MRS works have been published that based their spatial localization on CSI techniques. CSI is a phase-encoding technique that avoids the spatial misregistration of spectral signals that affect localization techniques based on frequency selective radiofrequency (RF) pulses in a constant gradient [9]. Aside from the improved signal localization, the CSI experiment can be designed to obtain the spatial distribution of spectra in localized volumes (voxels) in one, two, or three dimensions [3,9,10]. When ^{31}P MRS is acquired by means of three-dimensional (3D) CSI, the spectroscopic data can be prescribed and aligned in the three dimensions with anatomic features present in MR images by means of the voxel-shifting capability of the Fourier transform [10]. This means that exact preselection of the volume of interest is not necessary, which in turn simplifies data acquisition and reduces machine usage. An example of localized ^{31}P MRS of the human brain using 3D-CSI is shown in Fig. 3 (from [11]). After collecting reference images and adjusting the magnetic field shims, the 3D-CSI ^{31}P dataset was acquired and processed as described in the caption of Fig. 3. On the left of Fig. 3, a transverse MR image of the head has been overlaid with the corresponding localization grid of the CSI. In addition, spectra localized entirely in brain volumes (voxels) were subsampled and overlaid on the image. On the right of Fig. 3, the rightmost spectrum of the grid has been magnified. The quality of the localized spectra is indicated by the flat baseline, separation of the signals in the phosphomonoesters (Etn-P and Cho-P) and phosphodiesters (Gro-P-Etn and Gro-P-Cho) regions, and a signal-to-noise ratio (SNR) larger than 2 for the Pi signal.

3.2. Double-tuned coils

The low sensitivity of ^{31}P-MRS makes it important to obtain the highest SNR for its *in vivo* applications. This can be achieved, at least in part, by obtaining a highly homogeneous static magnetic field (B_0-field), which usually is adjusted using the ^{1}H water signal as a reference. Further, we have proved previously that some heteronuclear schemes enhance the *in vivo* sensitivity of ^{31}P signals by ^{1}H excitation (i.e., ^{1}H decoupling, nuclear Overhauser enhancement [NOE], and polarization transfer) [12,13]. We also have proved that, to obtain the most benefit from these heteronuclear schemes, the adjustment of the B_0-field needs to be thorough. We have developed a fast and reliable automated method for this based on ^{1}H CSI localization [14]. As stated before and shown in Figs 3 and 4, it also is necessary to collect ^{1}H MR images to anatomically place the *in vivo* localized ^{31}P signals. To facil-

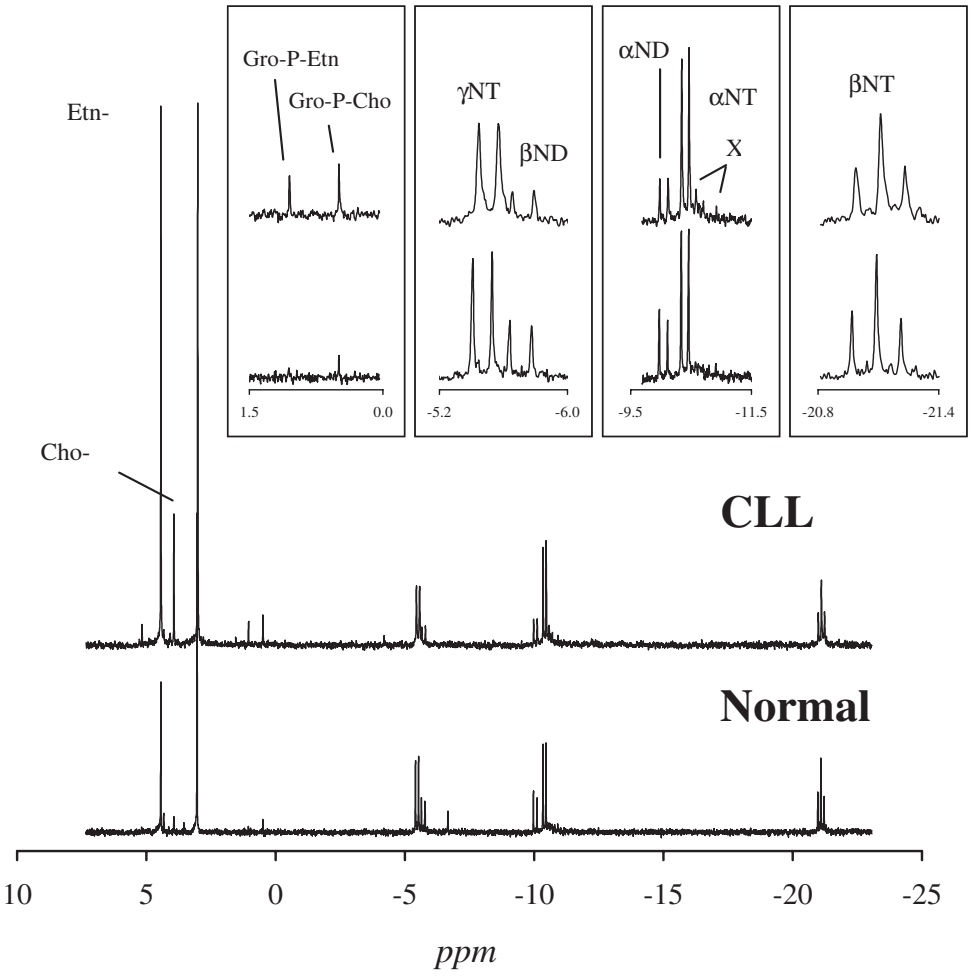

Fig. 1. ^{31}P MR spectroscopy of perchloric acid extracts of human lymphocytes. Examples of ^{31}P spectra from normal human lymphocytes (bottom spectrum; corrected pellet weight = 0.16 g) and chronic lymphocytic leukemia (CLL) lymphocytes (top spectrum; corrected pellet weight = 0.65 g) acquired and processed as described in [5]. ^{1}H-decoupled ^{31}P MR spectra were obtained at 25°C and 162 MHz (9.4 T). A 16 K free-induction decay (FID) was acquired in 1.02 s using a 45° pulse (8.6 μs), broadband composite-pulse ^{1}H-decoupling, and a total repetition time of 2.7 s. One to three 225-minute acquisitions with 5,000 transients were accumulated for each sample as needed to achieve an adequate signal-to-noise ratio. Chemical shifts (δ) were referenced to glycerophosphocholine (Gro-P-Cho; 0.494 ppm at pH 8.0). Considering that the concentration of nucleotide triphosphates (NTP) is constant in CLL and normal lymphocytes, the triplet of the β phosphate of NTP was used to scale the spectra (inset D) to ease comparisons. Due to the lower pellet weight and the scaling of the spectra, the noise in the normal lymphocyte spectrum appears larger. In the main panel, the signals of phosphoethanolamine (Etn-P) and phosphocholine (Cho-P) are labeled. The insets show expanded regions of the spectra. Inset A shows the region where the phosphodiester signals resonate (1.2–0.3 ppm). Glycerophospho-ethanolamine (Gro-P-Etn) and glycerophosphocholine (Gro-P-Cho) are labeled in the inset. Inset B shows the spectral region where the doublets of the terminal phosphates of the NTP (γ-NTP) and nucleotide diphosphates (NDP) moieties (β-NDP) resonate (-5.3 and -6.0 ppm), while inset C shows the region where the doublets of the α-phosphates from the NTP and NDP moieties resonate (-9.8 and -12.8 ppm). Several derivatives of diphosphonucleosides and diphospho-dinucleotides also resonate in the area shown in inset C (X and Y regions). Inset D shows the spectral region where the triplets of the β-phosphate of the NTP moieties resonate (-20.8 and -21.4 ppm).

itate all of these ^{1}H requirements during a ^{31}P study, our team designed several doublee-tuned RF antennas with highly sensitive ^{31}P and ^{1}H channels. Moreover, with these double-tuned antennas, ^{31}P and ^{1}H spectroscopy can be carried simultaneously, thereby minimizing adjustment and image requirements [15–17]. A comparison of the double-tuned probes with conventional, single-tuned ones showed that, despite double tuning, there is no significant loss in ^{31}P sensitivity when the ^{1}H channel provides the needed performance. For studies at 1.5 T, volume probes using a four-ring birdcage design were developed with the resonators operating in quadrature mode to provide improved sensitivity, excellent B1 homogeneity, and reduced pow-

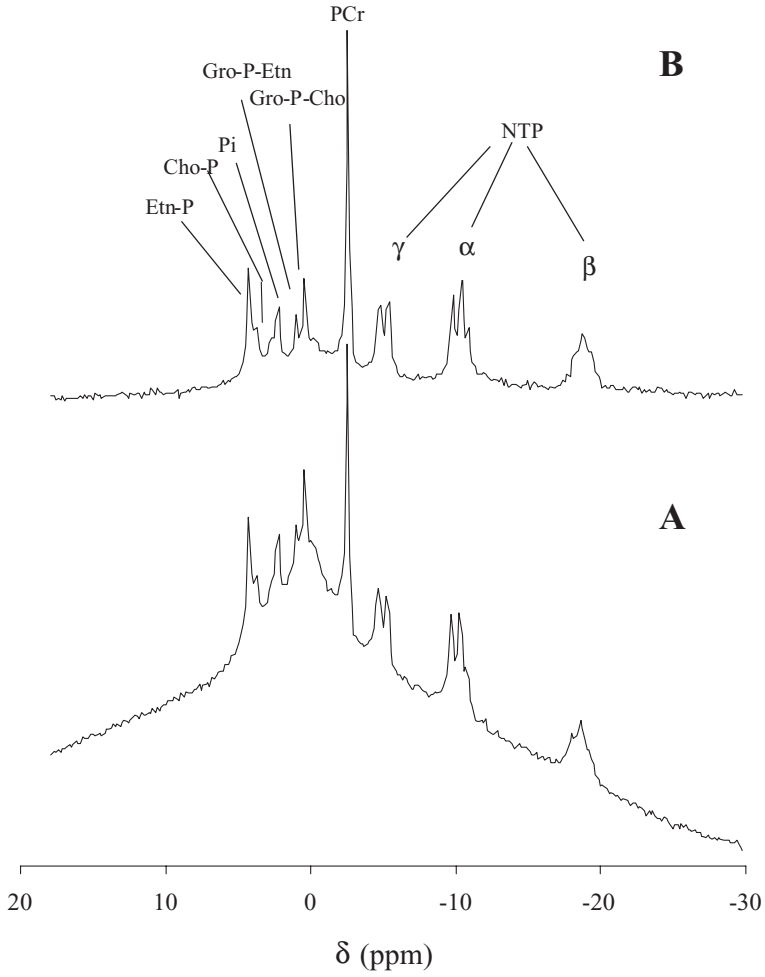

Fig. 2. ^{31}P MR spectroscopy from a normal human head. Proton-decoupled, NOE-enhanced ^{31}P spectra from a normal human head were collected at 1.5 T (TR = 1,000 ms, spectral width = ± 1,000 Hz, 256 acquisitions, and a 45° rectangular pulse). The chemical shift (δ) is expressed in parts-per-million (ppm), using phosphoric acid as the reference at 0 ppm (internal reference P_α of NTP at −10.01 ppm). Assignments: PCr, phosphocreatine, the rest as in Fig. 1. In spectrum A, the broad signal under the sharp resonance corresponds mainly to phospholipids. This broad signal was cancelled out during acquisition in spectrum B by applying an off-center Gaussian pulse (−300 Hz) that saturated this signal as described elsewhere [6].

er deposition at both frequencies [12]. Double-tuned surface coils with a flexible ^{1}H element also have been developed and used successfully by our group [18,19] and cooperatively by several institutions [20] to study superficial cancers in the trunk and extremities and triggered the development of a double-tuned surface probe specifically for the neck [21].

3.3. *Proton decoupling and nuclear Overhausser effect*

Simultaneous application of ^{1}H decoupling and NOE of *in vivo* ^{31}P signals significantly improves SNR and enhances spectral resolution [12]. We have acquired ^{1}H-decoupled, NOE-enhanced ^{31}P spectra localized to defined regions of different human tissues *in vivo* [12, 15,18,22]. The usual scheme to obtain ^{1}H-decoupled and fully NOE-enhanced ^{31}P spectra from human tissues *in vivo* includes the use of Waltz-4 modulation for proton decoupling and continuous wave bi-level excitation for NOE [12]. An example of the application of ^{1}H-decoupling and NOE to ^{31}P signals is shown in Fig. 4. Localized spectra of a non-Hodgkin's lymphoma tumor *in vivo* are shown before (lower spectrum) and after (upper spectrum) ^{1}H-decoupling and NOE were applied. Higher SNR and better resolved peaks in the phosphomonoester (Etn-P and Cho-P) and NTP regions were obtained in the ^{1}H-decoupled, NOE-

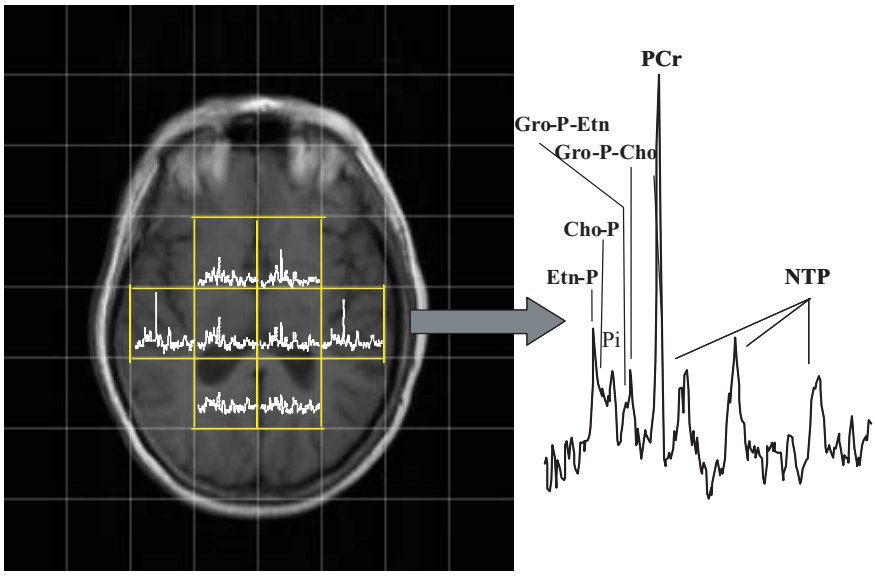

Fig. 3. Localized ^{31}P MR spectroscopy of a normal human head. On the left, a transverse MRI image of the head of a normal volunteer was overlaid with the ^{31}P CSI localization grid. The localized dataset was acquired as a cubic matrix with eight steps per spatial dimension with a nominal cubic voxel of 30 mm^3, field of view = 240 mm, TR = 1,000 ms, 512 points, spectral width of $\pm$1,000 Hz, four acquisitions per phase-encoding step, a 45° rectangular excitation pulse, and a Gaussian saturation pulse for PL as described in Fig. 2. The dataset was Fourier transformed in time and the three space dimensions, filtered with a Lorentzian waveform of 7 Hz, and globally phased. Non-contaminated brain spectra were subsampled and also are overlaid in the image. At the right of the figure, the rightmost spectrum on the grid was expanded to show spectral details. The spectral assignments are as described in Figs 1 and 2.

enhanced spectrum without processing for resolution ehancement. This demonstrates that ^{1}H-decoupling and NOE of ^{31}P signals permits obtaining more information about the *in vivo* metabolism of human tissues than was possible previously and should enhance the utility of this technique for studying human disorders.

4. In vivo markers of disease using ^{31}P MRS

Since the advent of larger bore spectrometers, human studies in healthy individuals have been carried out showing the usefulness of *in vivo* ^{31}P MRS to study normal muscle [23–33,4,35–53], liver [54,55], kidney [56], brain [4,7,57–62], testes [63], spleen [64], skin [65,66], heart [67,68], breast [69], uterus [70], and blood [71] and references therein. These studies have attempted to give actual molar concentration to phosphorus metabolites and magnesium, find metabolic fluxes of phosphorus compounds under particular conditions, and determine the normal intracellular pH values on the tissues studied. Examples of markers of disease using ^{31}P MRS can be found throughout the literature in which the levels of ^{31}P metabolites and/or their fluxes are modified due to specific illnesses. In vivo ^{31}P spectral alterations in acquired and genetic pathological human muscle conditions such as dermatomyositis and polymyositis [72], muscle dystrophies [73–76], ischemia [77], sporadic inclusion body myositis [78], progressive supranuclear palsy [79], malignant hyperthermia [80], fibromyalgia [81], pustular psoriasis [82], retinitis pigmentosa [83], Parkinson disease [84], McArdle's syndrome [85], adenylsuccinate lyase deficiency [86], hypo-ß-lipoproteinae mia [87], and some mitochondrial myopathies (cytochrome bc1 deficiency [88], carriers of 11778 mtDNA mutation [89], NARP syndrome [90], phosphofructokinase deficiency [91,92], Leber disease [93–95], and piruvate dehydrogenase complex deficiency [96] have been reported. The usual change found using ^{31}P MRS in these diseases is a reduction in the bioenergetics of the tissue. In addition, the effects of lipoic acid [97] and coenzyme Q_{10} [98,99] as treatment for mitochondrial cytopathies (MC) have been reported. Q_{10}has been shown to be especially promising for the treatment of mitochondrial diseases and perhaps for other diseases that involve compromised bioenergetics. The effects of thyroid hormones [100,101], insulin [102], exertional heatstroke [103], chronic fatigue syndrome [104], uremia [105], and phosphocreatine treatment [106] on muscle metabolism demonstrated by ^{31}P MR spectroscopy also have been reported.

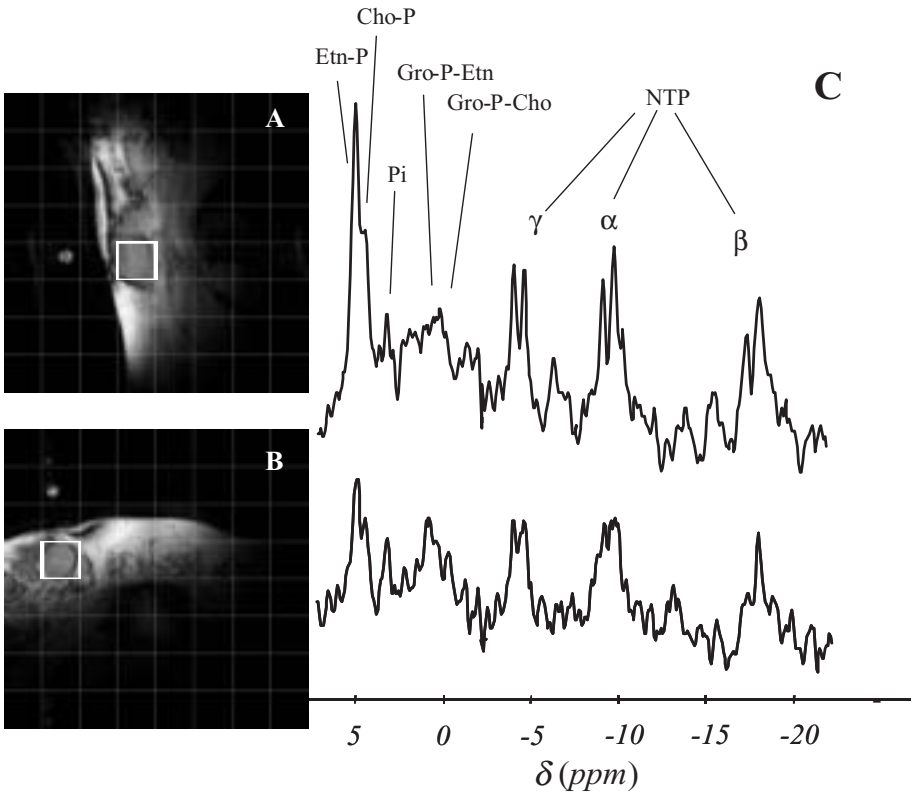

Fig. 4. Localized ^{31}P MR spectroscopy of a non-Hodgkin's lymphoma. Panels A and B show two orthogonal MR images (sagittal and transverse orientation, respectively), illustrating tumor localization, in this case in the right inguinal area. The images were overlaid with the ^{31}P 3D CSI localization grid. The ^{31}P spectra in panel C were sampled from the single tumor voxel projected on the images shown by a thick lined square. The localized ^{31}P datasets in this figure were acquired using the same parameters listed in the caption of Fig. 3, except for the off-center saturation. Proton-decoupling and NOE were applied only during the acquisition of the dataset from which the upper spectrum in panel C was sampled. The spectral assignments are as described in Figs 1 and 2.

In the brain, markers of disease have been demonstrated by ^{31}P MR spectroscopy in a number of organic diseases (i.e., seizures [107], neonatal intraventricular hemorrhage [108], migrane [109,110], head injury [111], lupus erythematosus [112], infarction [113], multiple sclerosis [114], hepatic encephalopathy [115], hydrocephalus [116], progressive supranuclear palsy [80], retinitis pigmentosa [83], epilepsia partialis continua [117], hypo-ß-lipoproteinaemia [87], cluster headache [118], and MC [89,95,119, 120]) as well as the brain effect of the treatment of MC with coenzyme Q_{10} [99]. Further, a group of diseases that have not been considered with a formal organic origin also have shown alteration on the *in vivo* ^{31}P MR spectroscopy of the brain usually characterized by changes in bioenergetics or phospholipid content (i.e., schizophrenia [121–130], bipolar disease [131–133], affective disorders [134], Alzheimer's disease [135–137], autism [138], depression [139], and dislexia [140]). Other human tissues with pathological conditions studied by *in vivo* ^{31}P MR spectroscopy have included liver (cirrhosis [141–145], diffuse hepatic disease [146], alcoholic disease [147–149], acute alcohol abstinence [150], hepatitis A infection [151], chronic hepatitis and its response to treatment [152], and the acute effect of ethanol and fructose [153]); bone (osteomalacia [154] and osteoporosis [155,156]); and heart (cardiomyopathy [157,158], coronary disease [158–160], mitral stenosis [161], and Friedreich ataxia [162] and its treatment with antioxidants [163]). Transplanted kidney [164,165] and psoriasis of the skin [166] also have been studied.

In vivo ^{31}P MR spectroscopy of human tumors deserves special consideration. The characteristic ^{31}P spectral pattern of tumors seen *in vitro*, which, unlike the majority of diseases studied is not related to bioenergetics but is instead related to modifications of intermediates of phospholipid metabolism, al-

so has been found *in vivo*. The pattern consists of relatively high concentrations of Etn-P and Cho-P. Several general reviews have been published on the subject [167–172], as well as papers on specific tumor histopathologies (lymphomas [173–176]; sarcomas [177–180]; and breast [69,181–185], lung [186, 187], brain [188], prostate [189], and liver carcinomas [190]) as well as follow up of anticancer treatment [191–195].

In the following sections, specific examples of the study of markers of disease using ^{31}P MR spectroscopy in MC, schizophrenia, non-Hodgkin's lymphoma, and chronic lymphocytic leukemia are described.

4.1. ^{31}P MRS studies in mitochondrial cytopathies

Due to their initial non-specific symptoms, differential diagnosis of MC must be done against the rest of the ailments grouped as neuromuscular diseases (ND). The ND group includes a variety of pathologies of acquired and genetic origin, common among children, with complicated identification and characterization due to overlapping clinical manifestations that delay instituting specific treatment. In the case of MC, the usual underlying alteration is a genetic mutation that produces malfunctions of the oxidative phosphorylation, with concomitant reductions in the cellular energy state. This energy deficit is demonstrated by decreased synthesis capacity for adenosine triphosphate (ATP, the most abundant intracellular NTP) by the respiratory chain, which in turn affects all tissues; especially those that are highly active (i.e., muscle, heart, nervous system). Although measurement of respiratory and phosphorylating activities in intact mitochondria isolated from the muscle of patients with ND is a very powerful *in vitro* method of identifying MC, the heterogeneity of these diseases can prevent their diagnosis using this methodology. It has been recognized that the non-invasive nature of ^{31}P MRS and its ability to visualize NTP, NDP, Pi, and PCr and their changes during exercise make it a promising technique to aid MC diagnosis and to monitor therapy [24,27,31,32,34,36,40,42,50,94,99, 196,198].

A simple protocol of *in vivo* ^{31}P MRS of active muscle can be used in the differential diagnosis of MC in pediatric patients with ND symptomatology. Under this protocol, we studied 23 ND-diagnosed patients (4–17 years-old) and 12 age-matched healthy volunteers with 100% compliance. Twelve of the ND patients already were confirmed as having MC based on isolated mitochondria studies and/or formal genetic determination of their mutation. The surface dual (^{1}H/^{31}P) antenna with flexible ^{1}H flaps described elsewhere [18] was wrapped around the right leg of the subjects using the sensitive field of the coil as the sole means for localization. Fifteen-second ^{31}P spectra of the right calf muscle acquired as described in the caption of Fig. 5 were collected serially before, during, and after calf activation (a 1-second plantar flexion/extension cycle against a mild resistance carried out continuously for 3 to 7 min). Intensity changes in Pi and PCr and chemical shifted changes in Pi related to pH always were recorded in all subjects, whereas no intensity changes in NTP were evident. The lack of changes in NTP was important for two reasons. One reason was to prevent strenuous exercise that could utilize NTP that in turn could generate pain and other discomforts; the other reason was to ensure that the muscle activation was not modifying the position of the RF antenna.

Under these exercise conditions, the PCr variations correspond to the usage of high-energy phosphates during the exercise period and their re-synthesis during post-exercise. Furthermore, the PCr re-synthesis post-exercise is proportional to the ATP synthesis by oxidative phosphorylation, which allows determination of the speed at which this pathway is working. Figure 5 shows an example of the spectroscopic results in one of the MC patients studied. While in this patient the PCr recovery curve took about 60 seconds from the exercise plateau to the baseline level, in normal volunteers this recovery was immediate ($>$ 15 sec). Slower recovery curves after exercise ($<$ 45 sec), such as the one shown in Fig. 5, were found in 9 of the 12 formally diagnosed MC patients, and fast (normal) recoveries ($>$ 25 sec) were found in 100% of normal volunteers. Furthermore, two previously undiagnosed ND patients also showed slower PCr recovery curves, despite normal results in their isolated mitochondria study. The possibility that these two ND patients could be suffering from MC but were missed by the isolated mitochondria study demonstrates the possible use of ^{31}P MR spectroscopy in the differential diagnosis of MC.

4.2. Brain studied by ^{31}P MRS in schizophrenia [11]

Changes in schizophrenia have suggested that the physiopathology of the disease probably is due to a low energy state in several areas of the brain. Accordingly, coenzyme Q_{10} (CoQ_{10}) has been hypothesized as improving brain energy states and cognitive functions in schizophrenia. We conducted a double-blind, placebo-controlled crossover study to examine the correlation

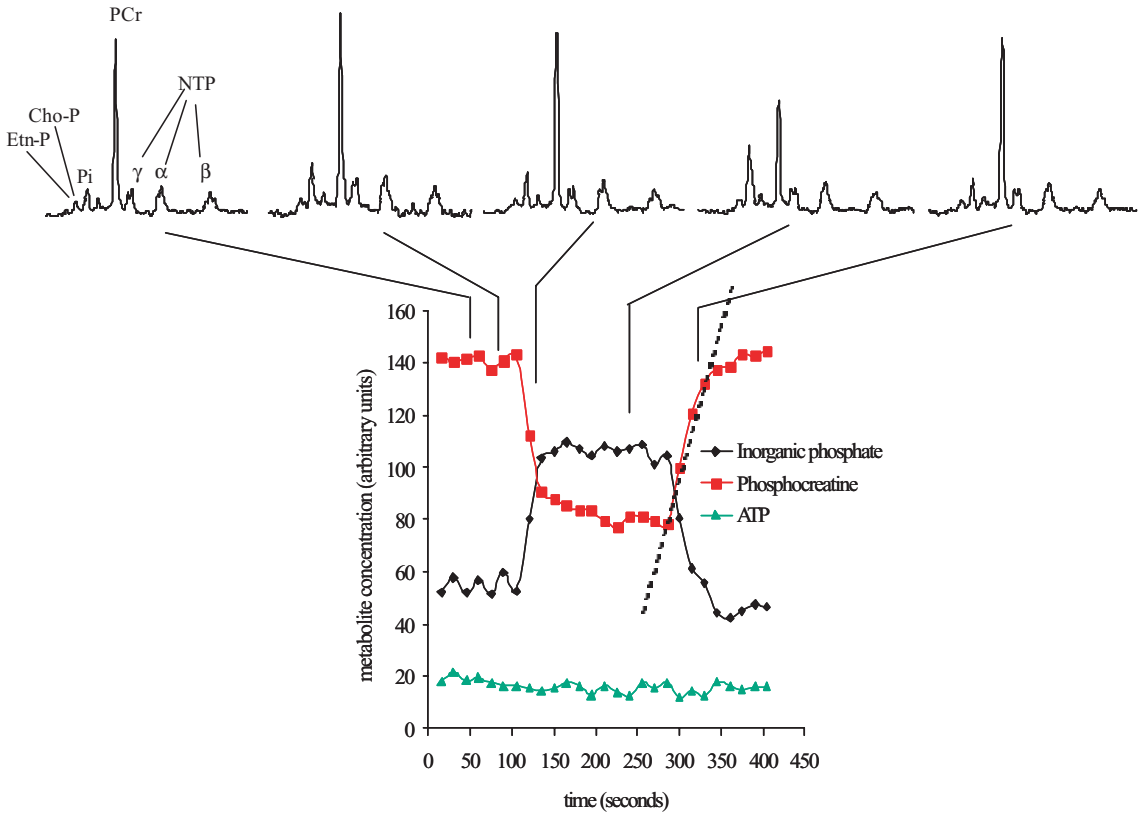

Fig. 5. Non-localized ^{31}P MR spectroscopy of calf muscle during activation. A series of spectra sampled from a muscle activation study carried out as described in the text is shown at the top of the figure. Each spectrum is a 15-second ^{1}H-decoupled, NOE-enhanced ^{31}P spectra of the right calf muscle (TR = 1s, 512 points spectral width of ±1,000 Hz, 15 acquisitions, and a 45° rectangular excitation pulse) collected serially before, during, and after calf activation. Spectral assignments are as described in Figs 1 and 2. The spectra on this figure show representative temporal changes in PCr and NTP during the activation protocol. The graph at the bottom of the figure shows the temporal changes in integration values of PCr (squares), Pi (diamonds), and ß-NTP (triangles) during the activation study. The dotted line corresponds to the PCr recovery after exercise which, under the conditions studied, is proportional to the ATP re-synthesis in the respiratory chain.

between cognitive results and the *in vivo* signals in brain-localized ^{31}P MRS, testing the effect of CoQ_{10} on impaired cognitive functions in schizophrenia patients under neuroleptic treatment. Ten schizophrenia patients were selected randomly to receive either placebo or CoQ_{10} during a period of 8 weeks, with the counterpart in the following 8 weeks. At the end of each arm, both cognitive studies and localized brain ^{31}P MRS were performed. However, only 7 of the 10 patients had the ^{31}P MRS studies done in both arms. Six matched normal volunteers also were used as controls for the brain ^{31}P MRS study.

The schizophrenia patients ($n = 10$) studied showed a slightly significant improvement in attention ($p \leqslant 0.05$) when treated with CoQ_{10} compared to placebo, but other cognitive tests failed to show differences for the group as a whole. When the patients were divided by below-normal (BN) and near-normal (NN) memory scores, a regular practice in schizophrenia research, the patients with BN scores ($n = 4$) showed significant improvement in verbal learning ($p \leqslant 0.01$), graph motor speed ($p \leqslant 0.04$), and attention ($p \leqslant 0.004$) during CoQ_{10} treatment. Patients with NN scores ($n = 6$) did not show significant changes in any of the cognitive studies during CoQ_{10} treatment.

Table 1 shows the mean brain PCr values obtained by ^{31}P MRS in the volunteer group ($n = 6$) and in the schizophrenia group ($n = 7$). As shown in the table, while on placebo, the schizophrenia group showed significantly lower brain PCr values than did normal volunteers ($p \leqslant 0.001$). The mean brain PCr value for schizophrenia patients increased significantly during the CoQ_{10} period ($p \leqslant 0.03$ against placebo), but this value still was significantly below that of the normal volunteers ($p \leqslant 0.03$). When the schizophrenia group was divided into BN ($n = 3$) and NN ($n = 4$) memo-

ry score subgroups, there was a significant increase in mean brain PCr value during CoQ_{10} treatment for the BN group ($p \leqslant 0.03$) and a non-significant increase for the NN group. We also analyzed these data on an individual basis, comparing the levels of PCr in the different voxels in each patient's brain during placebo or CoQ_{10} treatment. These results are shown in Fig. 6. In this analysis, two of the three patients in the BN subgroup showed statistically significant increases in PCr during CoQ_{10} treatment ($p \leqslant 0.001$ in both) with no changes in the third patient. The NN scores subgroup showed non-significant variations in PCr values.

The correlation of the cognitive studies with our ^{31}P MRS results suggests that the cognitive alterations found in schizophrenia may be explained at least in part by a problem in bioenergetics. In addition, the correlation between improvements in cognitive parameters and increased brain PCr levels in schizophrenia patients after CoQ_{10} treatment seen in this work also supports the link between a bioenergetic impairment and the low cognitive scores found in schizophrenia, a possible therapeutic use of CoQ_{10} for patients afflicted with schizophrenia, and the value of ^{31}P-MRS to follow up on these therapeutic changes.

4.3. Non-Hodgkin's lymphoma studies by in vivo ^{31}P MRS

Identification of metabolic or genetic variables from a tumor that correlate with success or failure of an individual treatment is of great clinical interest. Early knowledge of the likelihood of treatment failure would be of great use, because alternative therapies could then be considered. Currently, the commonly used indicator of treatment prognosis in non-Hodgkin's lymphomas (NHL) is the international prognostic index (IPI) [199, 200]. This index is based on clinical parameters related to tumor extent and host status and not to specific genetic or metabolic information about individual patients or their tumors.

Several groups have attempted to find tumor-specific genetic markers of disease in NHL to correlate with outcome in an attempt to determine whether such information improves prognostic accuracy beyond the IPI [201–207]. Non-genetic markers of disease in cancer also may be important to correlate with treatment response and outcome. In vivo ^{31}P MR spectroscopy of human tumors has shown a characteristic ^{31}P spectral pattern: the tumor levels of phospholipid-related phosphomonoesters, particularly Etn-P and Cho-P, have been known to be elevated in human tumors compared to most normal tissues since the first *in vivo* ^{31}P MRS observation of a rhabdomyosarcoma in the hand [208]. Several general reviews have been published on the subject [167–172], on specific tumor histopathologies [69, 173,190], and on specific treatments [191–195].

We have studied patients with NHL using localized ^{31}P MRS before treatment to demonstrate whether pretreatment levels of Etn-P plus Cho-P correlate with clinical parameters related to treatment response and outcome [19]. Three-dimensional, ^{1}H-decoupled, NOE-enhanced CSI of ^{31}P spectra was acquired from each patient's major tumor area in a 1.5 T clinical imager [10] using custom-built, dual-tuned (^{31}P/^{1}H) RF antennas, as described elsewhere [18,209]. The tumor-containing voxels in the CSI dataset were selected using the MR images as reference. Voxel-shifting [10] was used to reduce the amount of contamination in the tumor. An example of the procedure is shown in Fig. 4. Tumor voxels were extracted from the CSI datasets and summed when necessary to produce one spectrum per patient. The sum of the phosphate signals of the phospholipid-related phosphomonoesters, Etn-P and Cho-P (Etn-P+Cho-P), and the P_{β} signal of NTP in the resulting spectra were integrated manually to obtain the tumor [Etn-P+Cho-P]/NTP ratio. Each patient was studied in the 30 days prior to instituting a new treatment regimen. Treatments were at the discretion of the clinician. The response to treatment was determined following the World Health Organization criteria using bi-dimensional radiological measurements in serial CT scans.

We evaluated the pretreatment [Etn-P+Cho-P]/NTP levels in tumors for their ability to predict the patient's long-term (6-month) treatment response. Clinically, patients were classified into complete (CR) and not-complete responders (NCR). The difference between CR and NCR was significant (CR: 1.45 ± 0.15, mean $\pm$ standard error, $n = 10$ vs. NCR: 2.28 ± 0.15, $n = 17$, $p \leqslant 0.001$). A Fisher test for [Etn-P+Cho-P]/NTP also was significant (sensitivity = 70%, specificity = 71%, positive predictive value [PPV] of 58%, and overall accuracy = 70%, $p \leqslant 0.04$). When the patients were divided into risk groups depending on their IPI, the [Etn-P+Cho-P]/NTP ratio was significant for the low-risk (CR: 1.60 ± 0.21, mean $\pm$ standard error, $n = 5$ vs. NCR: 2.46 ± 0.25, $n = 6$; $p \leqslant 0.03$) and low-intermediate risk populations (CR: 1.30 ± 0.20, $n = 5$ vs. NCR: 2.20 ± 0.18, $n = 6$; $p \leqslant 0.01$). Using the average medians for CR and NCR of the low-risk group (1.99) and of the low-intermediate group (1.67), variable IPI-dependent cutoffs for [Etn-P+Cho-

Table 1
Brain Phosphocreatine Measured by ^{31}P MR Spectroscopy in Schizophrenia

Normal group ($n = 6$)	Brain PCr (arbitrary units)[a] 4.20 ± 0.16		Significance normal vs.		placebo vs. CoQ_{10}
Schizophrenia	placebo	CoQ_{10}	placebo	CoQ_{10}	
whole group ($n = 7$)	3.19 ± 0.18	3.59 ± 0.16	$p \leqslant 0.001$	$p \leqslant 0.03$	$p \leqslant 0.03$
below normal (BN) score group ($n = 3$)	2.99 ± 0.26	3.66 ± 0.34	$p \leqslant 0.003$	N.S.[b]	$p \leqslant 0.03$
near normal (NN) score group ($n = 4$)	3.39 ± 0.22	3.51 ± 0.09	$p \leqslant 0.02$	$p \leqslant 0.02$	N.S.

[a]Mean ± standard error.
[b]N.S., not significant.

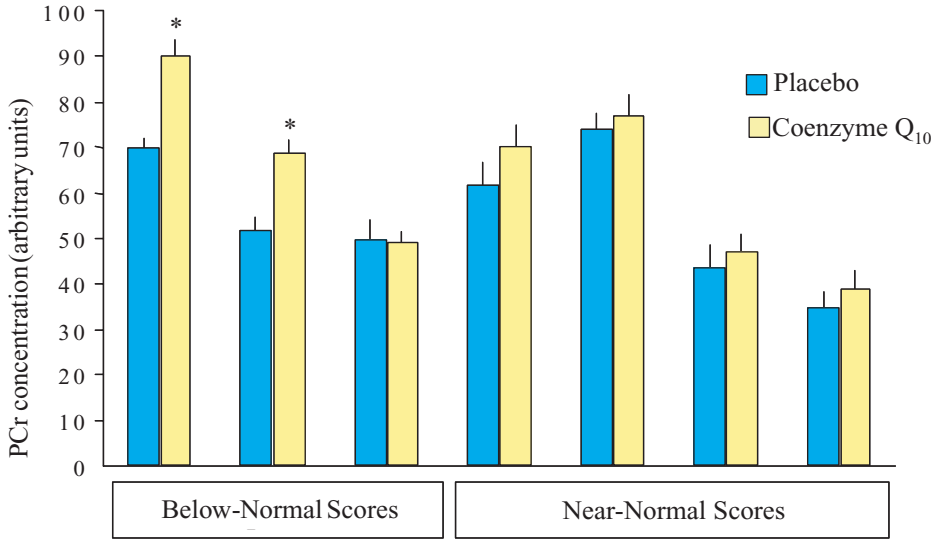

Fig. 6. Treatment response to coenzyme Q_{10} in schizophrenia. The brain PCr obtained using *in vivo* ^{31}P MR spectroscopy in each patient during placebo and Coenzyme Q_{10} (CoQ_{10}) as the mean ± standard error of the brain voxels selected are shown. Patients were segregated according to those with below-normal memory scores and those with near-normal memory scores. The two asterisks denote those brain PCr values during CoQ_{10} treatment that are significantly higher than those during placebo ($p \leqslant 0.001$ in both). As shown in the figure, the two significant PCr increases during CoQ_{10} treatment happened in patients with below-normal memory scores who were the patients with significant responses on the cognitive studies (see text).

P]/NTP were recognized that proved to be better predictors of long-term treatment response in a Fisher test. These variable cutoffs are such that, for patients at higher risk, with larger IPI values, a lower [Etn-P+Cho-P]/NTP is needed to predict positive outcome. Using these cutoffs, the Fisher test significance of the whole group increases to $p \leqslant 0.0002$, and its sensitivity and specificity improve to 80% and 94%, respectively.

These results suggest that we have identified an independent metabolic marker for disease. As far as we are aware, this is the first observation of an association between *in vivo* metabolite levels in tumors and clinical outcome, although genetic variations have been documented [207]. In any case, it is likely that, the more closely a variable can predict treatment outcome, the more likely the variable is causally connected to the underlying mechanism(s) responsible for the response to the treatment. This is true particularly when the variable is a specific intra-tumor metabolite or group of metabolites, as is the case in the present work. Thus, our results suggest that part of the metabolic pathway involved in a tumor being triggered into apoptosis is associated with the phospholipid precursors Etn-P and Cho-P. Although a detailed analysis of the causal possibilities is not feasible at present, the use of [Etn-P+Cho-P]/NTP levels in a clinical setting to guide therapy in individual patients appears to be possible once they have been confirmed in a larger patient cohort. In this work, we concluded that the pretreatment levels of Etn-P and Cho-P in NHL *in vivo* correlate with individual responses to treatment and time to treatment failure. This suggests that an independent factor in the variability of NHL tumor responses to therapy was identified and that it can be used as a predictor of treatment response.

4.4. Chronic lymphocytic leukemia studies by ^{31}P MRS [5]

Chronic lymphocytic leukemia (CLL) is a unique disease because it offers a link between *in vivo* and *in vitro* studies. CLL cells can be isolated easily from fresh blood so that cellular conditions are determined by the patient's clinical and treatment status, and cell extracts suitable for ^{31}P MRS analysis at high fields can be prepared immediately after isolation. Thus, the advantages associated with ^{31}P MRS studies of cultured cell lines can be obtained in a human tumor through *ex vivo* studies of CLL cell extracts. Furthermore, CLL and NHL both are B-lymphoid malignancies. The similar cellular origin of both tumors offers the possibility of comparing the *ex vivo* CLL results with our ongoing studies of NHL *in vivo*. In this preliminary CLL study, levels of phospholipid-related metabolites (Cho-P, Etn-P, Gro-P-Cho, Gro-P-Etn) of extracts from CLL leukemia lymphocytes and normal human lymphocytes were quantified using phosphorus MRS. Figure 1 shows an example of the comparison between normal (lower spectrum) and CLL lymphocytes (upper spectrum) in this study. The CLL cells vs. normal lymphocytes showed significant increases of Etn-P (8.11 ± 2.10 mean $\pm$ standard error, μmol/g wet weight, $n = 12$ vs. 3.63 ± 1.10, $n = 3$; $p \leqslant 0.002$), Cho-P (2.10 ± 0.37, $n = 12$ vs. 0.36 ± 0.09, $n = 3$; $p \leqslant 0.01$), Gro-P-Cho (0.26 ± 0.03, $n = 10$ vs. 0.11 ± 0.05, $n = 3$; $p \leqslant 0.004$), and Gro-P-Etn (0.33 ± 0.03, $n = 10$ vs. 0.17 ± 0.05, $n = 3$; $p \leqslant 0.003$). Further, the phospholipid precursor ethanolamine was studied in blood and was found to be reduced significantly in CLL patients (4.6 ± 1.6 μM, $n = 25$) compared to normal volunteers (7.7 ± 2.5, $n = 12$; $p \leqslant 0.001$). Increased intermediates with depletion of precursors suggest the presence of sustained phospholipid metabolism activation in CLL.

With respect to their ^{31}P MR spectra, CLL lymphocytes are characterized by elevated phosphomonoesters (Etn-P and Cho-P) and mobile phosphodiesters (Gro-P-Cho and Gro-P-Etn) in comparison to normal lymphocytes. This pattern of phospholipid-related metabolites cannot be accounted for by elevated serum ethanolamine. Although steady-state concentrations of Etn-P, Cho-P, Gro-P-Cho, Gro-P-Etn, CDP-ethanolamine, and CDP-choline are determined by a complex interaction of phospholipid synthetic pathways (from ethanolamine and choline), catabolic pathways (phospholipases A2, C, and D), and reentry of intermediates into synthetic pathways, probable causes for observed patterns can be inferred. For example, an increase of Gro-P-Etn and Gro-P-Cho upon mitogenic stimulation is compatible with a concurrent activation of phospholipase A2 known to occur upon stimulation [210,211]. Similar to mitogenically stimulated normal human lymphocytes, our study shows that CLL cells have higher Gro-P-Etn, CDP-ethanolamine, and Gro-P-Cho than controls, which suggests an activation of phospholipase A2 in CLL lymphocytes. Alternatively, activation of the kinases of ethanolamine and choline could be responsible for the elevated Etn-P and Cho-P seen in CLL cells if this activation is such that it compensates for lower substrate levels (lower serum ethanolamine in CLL patients than in controls).

A high concentration of Etn-P has been observed with stimulation of phospholipases C or D in a variety of cancer cell lines [212–214]. Gillham and Brindle suggested a tentative connection between the elevated levels of plasma fatty acids seen in cancer patients and the increased phosphomonoester signals observed in ^{31}P MR spectra of tumors [214]. Dixon and Tian in a murine lymphoma infiltrating the liver support this hypothesis of phospholipase C or D activation [215, 216]. In this tumor model, high Etn-P levels relative to Cho-P, and a lack of elevated Gro-P-Etn or Gro-P-Cho, were found. Etn-P synthesis was increased relative to that of Cho-P, and Etn-P synthesis via the CDP-ethanolamine synthetic pathway was decreased compared to the normal liver [215]. From these results, the authors suggested that their lymphoma model has high levels of Etn-P due to phospholipid breakdown via phospholipase C or D in combination with rate-limiting activity of CTP:Etn-P cytidylyltransferase [215]. Our results differ from these with regard to the elevation of Gro-P-Etn and Gro-P-Cho and a greater increase of Cho-P compared to Etn-P in CLL than in normal lymphocytes. Hence, we believe that sustained activation of phospholipase C or D is not the mechanism for our findings.

Although our data support phospholipase A2 or kinases activation in CLL, a formal mechanism by which these alterations are associated with malignancy still needs to be elucidated. However, regardless of the mechanism, there is a clear association between the malignant phenotype and elevated levels of Etn-P and Cho-P in both NHL and CLL cells. Moreover, several investigators have observed elevated levels of these compounds in other tumors as well [167,174,176,183, 215–231]. Since there is a reasonable possibility that this elevation is due to pathways that involve the control of fundamental cellular processes (such as apoptosis [232]), further investigation is warranted.

5. Summary

As illustrated above, there are many diseases in which the observation of *in vivo* metabolism can provide helpful clinical information, both for diagnosis and treatment. As our abilities to measure metabolites improve, these unique markers of disease, which clearly are related to the disease status in an individual patient, will become more useful in diagnosing and treating each unique patient.

Acknowledgements

The authors wish to thank all of their colleagues who have been involved in the work summarized in this publication (Radka Stoyanova, Suzanne Franks, Ronald McNamara, Francis Kappler, Frank Berardocco, Mitchell R. Smith, Ravi Srinivasan, Lynn Konchanin, Warren Grover, Agustin Leguido, Mary Selak) and those involved in the continuation of it (John R. Griffiths, Jason A. Koutcher, Martin O. Leach, Arend Heerschap, Jerry A. Glickson, Petra Kauffman, and Jaime Cruz-Lobo).

References

[1] S.R. Williams and D.G. Gadian, Tissue metabolism studied *in vivo* by nuclear magnetic resonance, *Q J Exp Physiol* **71**(3) (1986), 335–360.

[2] P.A. Bottomley, Spatial localization in NMR spectroscopy *in vivo*, *Ann N Y Acad Sci* **508** (1987), 333–348.

[3] T.R. Brown, B.M. Kincaid and K. Ugurbil, NMR chemical shift imaging in three dimensions, *Proc Natl Acad Sci USA* **79**(11) (1982), 3523–3526.

[4] H.S. Bachelard, D.W. Cox and P.G. Morris, Nuclear magnetic resonance as a tool to study brain metabolism, *Gerontology* **33**(3–4) (1987), 235–246.

[5] S.E. Franks, M.R. Smith and F. Arias-Mendoza, et al., Phosphomonoester concentrations differ between chronic lymphocytic leukemia cells and normal human lymphocytes, *Leuk Res* **26**(10) (2002), 919–926.

[6] R. McNamara, F. Arias-Mendoza and T.R. Brown, Investigation of broad resonances in ^{31}P NMR spectra of the human brain *in vivo*, *NMR Biomed* **7**(5) (1994), 237–242.

[7] J.W. Pettegrew, G. Withers, K. Panchalingam and J.F. Post, Considerations for brain pH assessment by ^{31}P NMR, *Magn Reson Imaging* **6**(2) (1988), 135–142.

[8] J.S. Taylor, D.B. Vigneron and J. Murphy-Boesch, et al., Free magnesium levels in normal human brain and brain tumors: ^{31}P chemical-shift imaging measurements at 1.5 T, *Proc Natl Acad Sci USA* **88**(15) (1991), 6810–6814.

[9] T.R. Brown, Practical applications of chemical shift imaging, *NMR Biomed* **5**(5) (1992), 238–243.

[10] D.B. Vigneron, S.J. Nelson and J. Murphy-Boesch, et al., Chemical shift imaging of human brain: axial, sagittal, and coronal P-31 metabolite images, *Radiology* **177**(3) (1990), 643–649.

[11] F. Arias-Mendoza, A. Elkashef, R. Stoyanova, J. Gold, R.J. Wyatt and T.R. Brown, Coenzyme Q_{10} effect on cognitive functions and bioenergetics in schizophrenia: a brain-localized ^{31}P MR spectroscopy study, in: *High power gradient MR-imaging, advances in MRI II*, M. Oudkerk and R.R. Edelman, eds, Berlin, Vienna: Blackwell Wissenschafts-Verlag, GmbH; 1997, pp. 257–262.

[12] J. Murphy-Boesch, R. Stoyanova and R. Srinivasan, et al., Proton-decoupled ^{31}P chemical shift imaging of the human brain in normal volunteers, *NMR Biomed* **6**(3) (1993), 173–180.

[13] O. Gonen, A. Mohebbi, R. Stoyanova and T.R. Brown, *In vivo* phosphorus polarization transfer and decoupling from protons in three-dimensional localized nuclear magnetic resonance spectroscopy of human brain, *Magn Reson Med* **37**(2) (1997), 301–306.

[14] J. Hu, T. Javaid, F. Arias-Mendoza, Z. Liu, R. McNamara and T.R. Brown, A fast, reliable, automatic shimming procedure using ^{1}H chemical-shift-imaging spectroscopy, *J Magn Reson B* **108**(3) (1995), 213–219.

[15] F. Arias-Mendoza, T. Javaid, R. Stoyanova, T.R. Brown and O. Gonen, Heteronuclear multivoxel spectroscopy of *in vivo* human brain: two-dimensional proton interleaved with three-dimensional ^{1}H-decoupled phosphorus chemical shift imaging, *NMR Biomed* **9**(3) (1996), 105–113.

[16] O. Gonen, J. Murphy-Boesch and R. Srinivasan, et al., Simultaneous and interleaved multinuclear chemical-shift imaging, a method for concurrent, localized spectroscopy, *J Magn Reson B* **104**(1) (1994), 26–33.

[17] O. Gonen, J. Hu, J. Murphy-Boesch, R. Stoyanova and T.R. Brown, Dual interleaved ^{1}H and proton-decoupled-^{31}P *in vivo* chemical shift imaging of human brain, *Magn Reson Med* **32**(1) (1994), 104–109.

[18] J. Murphy-Boesch, H. Jiang, R. Stoyanova and T.R. Brown, Quantification of phosphorus metabolites from chemical shift imaging spectra with corrections for point spread effects and B1 inhomogeneity, *Magn Reson Med* **39**(3) (1998), 429–438.

[19] F. Arias-Mendoza, M.R. Smith and T.R. Brown, Predicting treatment response in non-Hodgkin's lymphoma from pretreatment tumor content of phosphoethanolamine plus phosphocholine, *Acad Radiol* (2004), in press.

[20] J.R. Griffiths, A.R. Tate, F.A. Howe and M. Stubbs, Magnetic Resonance Spectroscopy of cancer-practicalities of multicentre trials and early results in non-Hodgkin's lymphoma, *Eur J Cancer* **38**(16) (2002), 2085.

[21] D.W. Klomp, D.J. Collins and H.J. van den Boogert, et al., Radio-frequency probe for ^{1}H decoupled ^{31}P MRS of the head and neck region, *Magn Reson Imaging* **19**(5) (2001), 755–759.

[22] C.W. Li, W.G. Negendank, J. Murphy-Boesch, K. Padavic-Shaller and T.R. Brown, Molar quantitation of hepatic metabolites *in vivo* in proton-decoupled, nuclear Overhauser effect enhanced ^{31}P NMR spectra localized by three-dimensional chemical shift imaging, *NMR Biomed* **9**(4) (1996), 141–155.

[23] D.J. Taylor, M. Crowe, P.J. Bore, P. Styles, D.L. Arnold and G.K. Radda, Examination of the energetics of aging skeletal muscle using nuclear magnetic resonance, *Gerontology* **30**(1) (1984), 2–7.

[24] P.A. Mole, R.L. Coulson, J.R. Caton, B.G. Nichols and T.J. Barstow, *In vivo* ^{31}P-NMR in human muscle: transient patterns with exercise, *J Appl Physiol* **59**(1) (1985), 101–104.
[25] W.R. Inch, B. Serebrin, A.W. Taylor and R.T. Thompson, Exercise muscle metabolism measured by magnetic resonance spectroscopy, *Can J Appl Sport Sci* **11**(2) (1986), 60–65.
[26] D.J. Taylor, P. Styles and P.M. Matthews, et al., Energetics of human muscle: exercise-induced ATP depletion, *Magn Reson Med* **3**(1) (1986), 44–54.
[27] A.A. Sapega, D.P. Sokolow, T.J. Graham and B. Chance, Phosphorus nuclear magnetic resonance: a non-invasive technique for the study of muscle bioenergetics during exercise, *Med Sci Sports Exerc* **19**(4) (1987), 410–420.
[28] C.A. Boicelli, A.M. Baldassarri, C. Borsetto and F. Conconi, An approach to noninvasive fiber type determination by NMR, *Int J Sports Med* **10**(1) (1989), 53–54.
[29] D. Rees, M.B. Smith, J. Harley and G.K. Radda, *In vivo* functioning of creatine phosphokinase in human forearm muscle, studied by ^{31}P NMR saturation transfer, *Magn Reson Med* **9**(1) (1989), 39–52.
[30] E. Achten, M. Van Cauteren and R. Willem, et al., ^{31}P-NMR spectroscopy and the metabolic properties of different muscle fibers, *J Appl Physiol* **68**(2) (1990), 644–649.
[31] D. Bendahan, S. Confort-Gouny, G. Kozak-Reiss and P.J. Cozzone, Heterogeneity of metabolic response to muscular exercise in humans. New criteria of invariance defined by *in vivo* phosphorus-31 NMR spectroscopy, *FEBS Lett* **272**(1–2) (1990), 155–158.
[32] S. Iotti, R. Funicello, P. Zaniol and B. Barbiroli, The rate of phosphate transport during recovery from muscular exercise depends on cytosolic [H^+]. A ^{31}P-MR spectroscopy study in humans, *Biochem Biophys Res Commun* **178**(3) (1991), 871–877.
[33] S. Iotti, R. Funicello, P. Zaniol and B. Barbiroli, Kinetics of post-exercise phosphate transport in human skeletal muscle: an *in vivo* ^{31}P-MR spectroscopy study, *Biochem Biophys Res Commun* **176**(3) (1991), 1204–1209.
[34] J.A. Jeneson, S.J. Nelson, D.B. Vigneron, J.S. Taylor, J. Murphy-Boesch and T.R. Brown, Two-dimensional ^{31}P-chemical shift imaging of intramuscular heterogeneity in exercising human forearm muscle, *Am J Physiol* **263**(2 Pt 1) (1992), C357–C364.
[35] G.K. Radda, Control, bioenergetics, and adaptation in health and disease: noninvasive biochemistry from nuclear magnetic resonance, *Faseb J* **6**(12) (1992), 3032–3038.
[36] S. Iotti, R. Lodi, C. Frassineti, P. Zaniol and B. Barbiroli, *In vivo* assessment of mitochondrial functionality in human gastrocnemius muscle by ^{31}P MRS. The role of pH in the evaluation of phosphocreatine and inorganic phosphate recoveries from exercise, *NMR Biomed* **6**(4) (1993), 248–253.
[37] G.J. Kemp, D.J. Taylor, P. Styles and G.K. Radda, The production, buffering and efflux of protons in human skeletal muscle during exercise and recovery, *NMR Biomed* **6**(1) (1993), 73–83.
[38] G.J. Kemp, D.J. Taylor and G.K. Radda, Control of phosphocreatine resynthesis during recovery from exercise in human skeletal muscle, *NMR Biomed* **6**(1) (1993), 66–72.
[39] G.J. Kemp, C.H. Thompson, P.R. Barnes and G.K. Radda, Comparisons of ATP turnover in human muscle during ischemic and aerobic exercise using ^{31}P magnetic resonance spectroscopy, *Magn Reson Med* **31**(3) (1994), 248–258.
[40] S. Kuno, H. Takahashi and K. Fujimoto, et al., Muscle metabolism during exercise using phosphorus-31 nuclear magnetic resonance spectroscopy in adolescents, *Eur J Appl Physiol Occup Physiol* **70**(4) (1995), 301–304.
[41] P.W. Hochachka, C.M. Clark, J.E. Holden, C. Stanley, K. Ugurbil and R.S. Menon, ^{31}P magnetic resonance spectroscopy of the Sherpa heart: a phosphocreatine/adenosine triphosphate signature of metabolic defense against hypobaric hypoxia, *Proc Natl Acad Sci USA* **93**(3) (1993), 1215–1220.
[42] G.K. Radda, Control of energy metabolism during muscle contraction, *Diabetes* **45**(1) (1996), S88–S92.
[43] T.W. Ryschon, D.L. Rosenstein, D.R. Rubinow, J.E. Niemela, R.J. Elin and R.S. Balaban, Relationship between skeletal muscle intracellular ionized magnesium and measurements of blood magnesium, *J Lab Clin Med* **127**(2) (1996), 207–213.
[44] H. Wackerhage, K. Mueller, U. Hoffmann, D. Leyk, D. Essfeld and J. Zange, Glycolytic ATP production estimated from ^{31}P magnetic resonance spectroscopy measurements during ischemic exercise *in vivo*, *Magma* **4**(3–4) (1996), 151–155.
[45] K.M. Ward, S.S. Rajan, M. Wysong, D. Radulovic and D.J. Clauw, Phosphorus nuclear magnetic resonance spectroscopy: *in vivo* magnesium measurements in the skeletal muscle of normal subjects, *Magn Reson Med* **36**(3) (1996), 475–480.
[46] P.S. Allen, G.O. Matheson and G. Zhu, et al., Simultaneous ^{31}P MRS of the soleus and gastrocnemius in Sherpas during graded calf muscle exercise, *Am J Physiol* **273**(3 Pt 2) (1997), R999–R1007.
[47] K.E. Conley, M.L. Blei, T.L. Richards, M.J. Kushmerick and S.A. Jubrias, Activation of glycolysis in human muscle *in vivo*, *Am J Physiol* **273**(1 Pt 1) (1997), C306–C315.
[48] J. Mizrahi, D. Seelenfreund, E. Isakov and Z. Susak, Predicted and measured muscle forces after recoveries of differing durations following fatigue in functional electrical stimulation, *Artif Organs* **21**(3) (1997), 236–239.
[49] R. Roussel, P.G. Carlier, J.J. Robert, G. Velho and G. Bloch, ^{13}C/^{31}P NMR studies of glucose transport in human skeletal muscle, *Proc Natl Acad Sci USA* **95**(3) (1998), 1313–1318.
[50] D. Sappey-Marinier, A. Dheyriat, M. Lissac, J. Frutoso, J.J. Mallet and A. Bonmartin, A metabolism study of human masseter muscle by ^{31}P magnetic resonance spectroscopy during long periods of exercise and recovery, *Eur J Oral Sci* **106**(1) (1998), 552–558.
[51] R. Buchli and P. Boesiger, Comparison of methods for the determination of absolute metabolite concentrations in human muscles by ^{31}P MRS, *Magn Reson Med* **30**(5) (1993), 552–558.
[52] A.A. Sapega, D.P. Sokolow, T.J. Graham and B. Chance, Phosphorus nuclear magnetic resonance: a non-invasive technique for the study of muscle bioenergetics during exercise, *Med Sci Sports Exerc* **25**(6) (1993), 656–666.
[53] S. Iotti, R. Lodi, G. Gottardi, P. Zaniol and B. Barbiroli, Inorganic phosphate is transported into mitochondria in the absence of ATP biosynthesis: an *in vivo* ^{31}P NMR study in the human skeletal muscle, *Biochem Biophys Res Commun* **225**(1) (1996), 191–194.
[54] R.D. Oberhaensli, G.J. Galloway, D.J. Taylor, P.J. Bore and G.K. Radda, Assessment of human liver metabolism by phosphorus-31 magnetic resonance spectroscopy, *Br J Radiol* **59**(703) (1986), 695–699.
[55] P.C. Dagnelie, D.K. Menon and I.J. Cox, et al., Effect of L-alanine infusion on ^{31}P nuclear magnetic resonance spectra of normal human liver: towards biochemical pathology *in vivo*, *Clin Sci* (*Lond*) **83**(2) (1992), 183–190.

[56] B. Ross, D. Freeman and L. Chan, Contributions of nuclear magnetic resonance to renal biochemistry, *Kidney Int* **29**(1) (1986), 131–141.
[57] D.P. Younkin, M. Delivoria-Papadopoulos and J.C. Leonard, et al., Unique aspects of human newborn cerebral metabolism evaluated with phosphorus nuclear magnetic resonance spectroscopy, *Ann Neurol* **16**(5) (1984), 581–586.
[58] P.A. Bottomley, H.C. Charles and P.B. Roemer, et al., Human *in vivo* phosphate metabolite imaging with ^{31}P NMR, *Magn Reson Med* **7**(3) (1988), 319–336.
[59] H.R. Halvorson, A.M. Vande Linde, J.A. Helpern and K.M. Welch, Assessment of magnesium concentrati ons by ^{31}P NMR *in vivo*, *NMR Biomed* **5**(2) (1992), 53–58.
[60] W. Hemmer and T. Wallimann, Functional aspects of creatine kinase in brain, *Dev Neurosci* **15**(3–5) (1993), 249–260.
[61] R. Buchli, E. Martin, P. Boesiger and H. Rumpel, Developmental changes of phosphorus metabolite concentrations in the human brain: a ^{31}P magnetic resonance spectroscopy study *in vivo*, *Pediatr Res* **35**(4 Pt 1) (1994), 431–435.
[62] E.F. Jackson and C.A. Meyers, Introduction to hippocampal spectroscopy, *Neuroimaging Clin N Am* **7**(1) (1997), 143–154.
[63] W.M. Chew and H. Hricak, Phosphorus-31 MRS of human testicular function and viability, *Invest Radiol* **24**(12) (1989), 997–1000.
[64] S.R. Smith, P.A. Martin, J.M. Davies and R.H. Edwards, Characterization of the spleen by *in vivo* image guided ^{31}P magnetic resonance spectroscopy, *NMR Biomed* **2**(4) (1989), 172–178.
[65] A. Zemtsov, T.C. Ng and M. Xue, Human *in vivo* ^{31}P spectroscopy of skin: potentially a powerful tool for noninvasive study of metabolism in a cutaneous tissue, *J Dermatol Surg Oncol* **15**(11) (1989), 1207–1211.
[66] A.G. Cowie, M.E. Bastin, D.N. Manners, L.J. Hands, P. Styles and G.K. Radda, ^{31}P NMR studies of human skin using a modified zig-zag surface coil, *NMR Biomed* **9**(5) (1996), 195–200.
[67] P.A. Bottomley, C.J. Hardy and P.B. Roemer, Phosphate metabolite imaging and concentration measurements in human heart by nuclear magnetic resonance, *Magn Reson Med* **14**(3) (1990), 425–434.
[68] S. Kuno, T. Ogawa, S. Katsuta and Y. Itai, *In vivo* human myocardial metabolism during aerobic exercise by phosphorus-31 nuclear magnetic resonance spectroscopy, *Eur J Appl Physiol Occup Physiol* **69**(6) (1994), 488–491.
[69] C.J. Twelves, M. Lowry and D.A. Porter, et al., Phosphorus-31 metabolism of human breast-an *in vivo* magnetic resonance spectroscopic study at 1.5 Tesla, *Br J Radiol* **67**(793) (1994), 36–45.
[70] T. Steingrimsdottir, A. Ericsson, A. Franck, A. Waldenstrom, U. Ulmsten and G. Ronquist, Human uterine smooth muscle exhibits a very low phosphocreatine/ATP ratio as assessed by *in vitro* and *in vivo* measurements, *Eur J Clin Invest* **27**(9) (1997), 743–749.
[71] M. Horn, M. Madgien, K. Schnackerz and S. Neubauer, ^{31}P-nuclear magnetic resonance spectroscopy of blood: a species comparison, *J Cardiovasc Magn Reson* **2**(2) (2000), 143–149.
[72] G. Cea, D. Bendahan and D. Danners, et al., Reduced oxidative phosphorylation and proton efflux suggest reduced capillary blood supply in skeletal muscle of patients with dermatomyositis and polymyositis: a quantitative ^{31}P-magnetic resonance spectroscopy and MRI study, *Brain* **125**(Pt 7) (2002), 1635–1645.
[73] R.J. Newman, An *in vivo* study of muscle phosphate metabolism in Becker's dystrophy by ^{31}P NMR spectroscopy, *Metabolism* **34**(8) (1985), 737–740.
[74] B. Barbiroli, K.K. McCully, S. Iotti, R. Lodi, P. Zaniol and B. Chance, Further impairment of muscle phosphate kinetics by lengthening exercise in DMD/BMD carriers. An *in vivo* ^{31}P-NMR spectroscopy study, *J Neurol Sci* **119**(1) (1993), 65–73.
[75] H. Ikehira, S. Nishikawa, K. Matsumura, T. Hasegawa, N. Arimizu and Y. Tateno, The functional staging of Duchenne muscular dystrophy using *in vivo* ^{31}P MR spectroscopy, *Radiat Med* **13**(2) (1995), 63–65.
[76] R. Lodi, G.J. Kemp and F. Muntoni, et al., Reduced cytosolic acidification during exercise suggests defective glycolytic activity in skeletal muscle of patients with Becker muscular dystrophy. An *in vivo* ^{31}P magnetic resonance spectroscopy study, *Brain* **122**(Pt 1) (1999), 121–130.
[77] M.A. Zatina, H.D. Berkowitz, G.M. Gross, J.M. Maris and B. Chance, ^{31}P nuclear magnetic resonance spectroscopy: noninvasive biochemical analysis of the ischemic extremity, *J Vasc Surg* **3**(3) (1986), 411–420.
[78] R. Lodi, D.J. Taylor and S.J. Tabrizi, et al., Normal *in vivo* skeletal muscle oxidative metabolism in sporadic inclusion body myositis assessed by ^{31}P-magnetic resonance spectroscopy, *Brain* **121**(Pt 11) (1998), 2119–2126.
[79] P. Martinelli, C. Scaglione, R. Lodi, S. Iotti and B. Barbiroli, Deficit of brain and skeletal muscle bioenergetics in progressive supranuclear palsy shown *in vivo* by phosphorus magnetic resonance spectroscopy, *Mov Disord* **15**(5) (2000), 889–893.
[80] J.F. Payen, J.L. Bosson and L. Bourdon, et al., Improved noninvasive diagnostic testing for malignant hyperthermia susceptibility from a combination of metabolites determined *in vivo* with ^{31}P-magnetic resonance spectroscopy, *Anesthesiology* **78**(5) (1993), 848–855.
[81] A.C. de Blecourt, R.F. Wolf, M.H. van Rijswijk, R.L. Kamman, A.A. Knipping and E.L. Mooyaart, *In vivo* ^{31}P magnetic resonance spectroscopy (MRS) of tender points in patients with primary fibromyalgia syndrome, *Rheumatol Int* **11**(2) (1991), 51–54.
[82] I.C. Kiricuta, S. el-Gammal, P. Altmeyer and H.K. Beyer, Altered muscle metabolism in pustular psoriasis (Zumbusch type): demonstration by ^{31}P magnetic resonance spectroscopy, *Dermatology* **186**(3) (1993), 170–175.
[83] R. Lodi, S. Iotti and L. Scorolli, et al., The use of phosphorus magnetic resonance spectroscopy to study *in vivo* the effect of coenzyme Q_{10} treatment in retinitis pigmentosa, *Mol Aspects Med* **15** (1994), s221–s230.
[84] D.J. Taylor, D. Krige and P.R. Barnes, et al., A ^{31}P magnetic resonance spectroscopy study of mitochondrial function in skeletal muscle of patients with Parkinson's disease, *J Neurol Sci* **125**(1) (1994), 77–81.
[85] Z. Argov, W.J. Bank, J. Maris and B. Chance, Muscle energy metabolism in McArdle's syndrome by *in vivo* phosphorus magnetic resonance spectroscopy, *Neurology* **37**(11) (1987), 1720–1724.
[86] C. Salerno, S. Iotti, R. Lodi, C. Crifo and B. Barbiroli, Failure of muscle energy metabolism in a patient with adenylosuccinate lyase deficiency. An *in vivo* study by phosphorus NMR spectroscopy, *Biochim Biophys Acta* **1360**(3) (1997), 271–276.
[87] R. Lodi, R. Rinaldi and A. Gaddi, et al., Brain and skeletal muscle bioenergetic failure in familial hypobetalipopro-

teinaemia, *J Neurol Neurosurg Psychiatry* **62**(6) (1997), 574–580.

[88] N.G. Kennaway, Defects in the cytochrome bc1 complex in mitochondrial diseases, *J Bioenerg Biomembr* **20**(3) (1988), 325–352.

[89] B. Barbiroli, P. Montagna and P. Cortelli, et al., Defective brain and muscle energy metabolism shown by *in vivo* ^{31}P magnetic resonance spectroscopy in nonaffected carriers of 11778 mtDNA mutation, *Neurology* **45**(7) (1995), 1364–1369.

[90] R. Lodi, P. Montagna and S. Iotti, et al., Brain and muscle energy metabolism studied *in vivo* by ^{31}P-magnetic resonance spectroscopy in NARP syndrome, *J Neurol Neurosurg Psychiatry* **57**(12) (1994), 1492–1496.

[91] G.M. Fabrizi, R. Lodi and M. D'Ettorre, et al., Autosomal dominant limb girdle myopathy with ragged-red fibers and cardiomyopathy. A pedigree study by *in vivo* ^{31}P-MR spectroscopy indicating a multisystem mitochondrial defect, *J Neurol Sci* **137**(1) (1996), 20–27.

[92] R. Massa, R. Lodi and B. Barbiroli, et al., Partial block of glycolysis in late-onset phosphofructokinase deficiency myopathy, *Acta Neuropathol* (*Berl*) **91**(3) (1996), 322–329.

[93] P. Cortelli, P. Montagna and G. Pierangeli, et al., Clinical and brain bioenergetics improvement with idebenone in a patient with Leber's hereditary optic neuropathy: a clinical and ^{31}P-MRS study, *J Neurol Sci* **148**(1) (1997), 25–31.

[94] R. Lodi, D.J. Taylor and S.J. Tabrizi, et al., *In vivo* skeletal muscle mitochondrial function in Leber's hereditary optic neuropathy assessed by ^{31}P magnetic resonance spectroscopy, *Ann Neurol* **42**(4) (1997), 573–579.

[95] R. Lodi, V. Carelli and P. Cortelli, et al., Phosphorus MR spectroscopy shows a tissue specific *in vivo* distribution of biochemical expression of the G3460A mutation in Leber's hereditary optic neuropathy, *J Neurol Neurosurg Psychiatry* **72**(6) (2002), 805–807.

[96] C. Marsac, D. Stansbie and G. Bonne, et al., Defect in the lipoyl-bearing protein X subunit of the pyruvate dehydrogenase complex in two patients with encephalomyelopathy, *J Pediatr* **123**(6) (1993), 915–920.

[97] B. Barbiroli, R. Medori and H.J. Tritschler, et al., Lipoic (thioctic) acid increases brain energy availability and skeletal muscle performance as shown by *in vivo* ^{31}P-MRS in a patient with mitochondrial cytopathy, *J Neurol* **242**(7) (1995), 472–477.

[98] B. Barbiroli, C. Frassineti and P. Martinelli, et al., Coenzyme Q_{10} improves mitochondrial respiration in patients with mitochondrial cytopathies. An *in vivo* study on brain and skeletal muscle by phosphorous magnetic resonance spectroscopy, *Cell Mol Biol* (*Noisy-le-grand*) **43**(5) (1997), 741–749.

[99] B. Barbiroli, S. Iotti and R. Lodi, Improved brain and muscle mitochondrial respiration with CoQ. An *in vivo* study by ^{31}P-MR spectroscopy in patients with mitochondrial cytopathies, *Biofactors* **9**(2–4) (1999), 253–260.

[100] Z. Argov, P.F. Renshaw, B. Boden, A. Winokur and W.J. Bank, Effects of thyroid hormones on skeletal muscle bioenergetics. In vivo phosphorus-31 magnetic resonance spectroscopy study of humans and rats, *J Clin Invest* **81**(6) (1988), 1695–1701.

[101] M. Erkintalo, D. Bendahan, J.P. Mattei, C. Fabreguettes, P. Vague and P.J. Cozzone, Reduced metabolic efficiency of skeletal muscle energetics in hyperthyroid patients evidenced quantitatively by *in vivo* phosphorus-31 magnetic resonance spectroscopy, *Metabolism* **47**(7) (1998), 769–776.

[102] D.J. Taylor, S.W. Coppack and T.A. Cadoux-Hudson, et al., Effect of insulin on intracellular pH and phosphate metabolism in human skeletal muscle *in vivo*, *Clin Sci* (*Lond*) **81**(1) (1991), 123–128.

[103] J.F. Payen, L. Bourdon and H. Reutenauer, et al., Exertional heatstroke and muscle metabolism: an *in vivo* ^{31}P-MRS study, *Med Sci Sports Exerc* **24**(4) (1992), 420–425.

[104] R. Wong, G. Lopaschuk and G. Zhu, et al., Skeletal muscle metabolism in the chronic fatigue syndrome. *In vivo* assessment by ^{31}P nuclear magnetic resonance spectroscopy, *Chest* **102**(6) (1992), 1716–1722.

[105] P. Taborsky, I. Sotornik, J. Kaslikova, O. Schuck, M. Hajek and A. Horska, ^{31}P magnetic resonance spectroscopy investigation of skeletal muscle metabolism in uraemic patients, *Nephron* **65**(2) (1993), 222–226.

[106] C. Frassineti, S. Iotti, R. Lodi, P. Zaniol and B. Barbiroli, Effect of oral phosphocreatinine on human skeletal muscle shown by *in vivo* ^{31}P-NMR, *In Vivo* **10**(4) (1996), 429–433.

[107] D.P. Younkin, M. Delivoria-Papadopoulos, J. Maris, E. Donlon, R. Clancy and B. Chance, Cerebral metabolic effects of neonatal seizures measured with *in vivo* ^{31}P NMR spectroscopy, *Ann Neurol* **20**(4) (1986), 513–519.

[108] D. Younkin, B. Medoff-Cooper, R. Guillet, T. Sinwell, B. Chance and M. Delivoria-Papadopoulos, *In vivo* ^{31}P nuclear magnetic resonance measurement of chronic changes in cerebral metabolites following neonatal intraventricular hemorrhage, *Pediatrics* **82**(3) (1988), 331–336.

[109] N.M. Ramadan, H. Halvorson, A. Vande-Linde, S.R. Levine, J.A. Helpern and K.M. Welch, Low brain magnesium in migraine, *Headache* **29**(9) (1989), 590–593.

[110] R. Lodi, P. Montagna and S. Soriani, et al., Deficit of brain and skeletal muscle bioenergetics and low brain magnesium in juvenile migraine: an *in vivo* ^{31}P magnetic resonance spectroscopy interictal study, *Pediatr Res* **42**(6) (1997), 866–871.

[111] T.A. Cadoux-Hudson, D. Wade and D.J. Taylor, et al., Persistent metabolic sequelae of severe head injury in humans *in vivo*, *Acta Neurochir* (*Wien*) **104**(1–2) (1990), 1–7.

[112] R.H. Griffey, M.S. Brown, A.D. Bankhurst, R.R. Sibbitt and W.L. Sibbitt, Jr. Depletion of high-energy phosphates in the central nervous system of patients with systemic lupus erythematosus, as determined by phosphorus-31 nuclear magnetic resonance spectroscopy, *Arthritis Rheum* **33**(6) (1990), 827–833.

[113] M. Sasahira, K. Uchimura, K. Yatsushiro, T. Fujimoto and T. Asakura, Early detection of cerebral infarction by ^{31}P spectroscopic imaging, *Neuroradiology* **32**(1) (1990), 43–46.

[114] C.A. Husted, D.S. Goodin and J.W. Hugg, et al., Biochemical alterations in multiple sclerosis lesions and normal-appearing white matter detected by *in vivo* ^{31}P and ^{1}H spectroscopic imaging, *Ann Neurol* **36**(2) (1994), 157–165.

[115] S.D. Taylor-Robinson, C. Buckley, K.K. Changani, H.J. Hodgson and J.D. Bell, Cerebral proton and phosphorus-31 magnetic resonance spectroscopy in patients with subclinical hepatic encephalopathy, *Liver* **19**(5) (1999), 389–398.

[116] K.P. Braun, W.P. Vandertop, R.H. Gooskens, K.A. Tulleken and K. Nicolay, NMR spectroscopic evaluation of cerebral metabolism in hydrocephalus: a review, *Neurol Res* **22**(1) (2000), 51–64.

[117] C. Antozzi, S. Franceschetti and G. Filippini, et al., Epilepsia partialis continua associated with NADH-coenzyme Q reductase deficiency, *J Neurol Sci* **129**(2) (1995), 152–161.

[118] P. Montagna, R. Lodi and P. Cortelli, et al., Phosphorus magnetic resonance spectroscopy in cluster headache, *Neurology* **48**(1) (1997), 113–118.
[119] B. Barbiroli, P. Montagna and P. Martinelli, et al., Defective brain energy metabolism shown by *in vivo* ^{31}P MR spectroscopy in 28 patients with mitochondrial cytopathies, *J Cereb Blood Flow Metab* **13**(3) (1993), 469–474.
[120] B. Barbiroli, S. Iotti and P. Cortelli, et al., Low brain intracellular free magnesium in mitochondrial cytopathies, *J Cereb Blood Flow Metab* **19**(5) (1999), 528–532.
[121] T. Fujimoto, T. Nakano, T. Takano, Y. Hokazono, T. Asakura and T. Tsuji, Study of chronic schizophrenics using ^{31}P magnetic resonance chemical shift imaging, *Acta Psychiatr Scand* **86**(6) (1992), 455–462.
[122] J.W. Pettegrew, M.S. Keshavan and N.J. Minshew, ^{31}P nuclear magnetic resonance spectroscopy: neurodevelopment and schizophrenia, *Schizophr Bull* **19**(1) (1993), 35–53.
[123] R.F. Deicken, G. Calabrese and E.L. Merrin, et al., 31phosphorus magnetic resonance spectroscopy of the frontal and parietal lobes in chronic schizophrenia, *Biol Psychiatry* **36**(8) (1994), 503–510.
[124] R.F. Deicken, G. Calabrese, E.L. Merrin, S. Vinogradov, G. Fein and M.W. Weiner, Asymmetry of temporal lobe phosphorous metabolism in schizophrenia: a 31phosphorous magnetic resonance spectroscopic imaging study, *Biol Psychiatry* **38**(5) (1995), 279–286.
[125] R.F. Deicken, G. Calabrese, E.L. Merrin, G. Fein and M.W. Weiner, Basal ganglia phosphorous metabolism in chronic schizophrenia, *Am J Psychiatry* **152**(1) (1995), 126–129.
[126] P.C. Williamson, M. Brauer, S. Leonard, T. Thompson and D. Drost, ^{31}P magnetic resonance spectroscopy studies in schizophrenia, *Prostaglandins Leukot Essent Fatty Acids* **55**(1–2) (1996), 115–118.
[127] S. Bluml, J. Tan and K. Harris, et al., Quantitative proton-decoupled ^{31}P MRS of the schizophrenic brain *in vivo*, *J Comput Assist Tomogr* **23**(2) (1999), 272–275.
[128] H. Fukuzako, T. Fukuzako, T. Hashiguchi, S. Kodama, M. Takigawa and T. Fujimoto, Changes in levels of phosphorus metabolites in temporal lobes of drug-naive schizophrenic patients, *Am J Psychiatry* **156**(8) (1999), 1205–1208.
[129] J.J. Potwarka, D.J. Drost and P.C. Williamson, et al., A ^{1}H-decoupled ^{31}P chemical shift imaging study of medicated schizophrenic patients and healthy controls, *Biol Psychiatry* **45**(6) (1999), 687–693.
[130] T. Shioiri, H. Hamakawa and T. Kato, et al., Frontal lobe membrane phospholipid metabolism and ventricle to brain ratio in schizophrenia: preliminary ^{31}P-MRS and CT studies, *Eur Arch Psychiatry Clin Neurosci* **250**(4) (2000), 169–174.
[131] T. Kato, T. Shioiri, S. Takahashi and T. Inubushi, Measurement of brain phosphoinositide metabolism in bipolar patients using *in vivo* ^{31}P-MRS, *J Affect Disord* **22**(4) (1991), 185–190.
[132] T. Kato, S. Takahashi, T. Shioiri and T. Inubushi, Alterations in brain phosphorous metabolism in bipolar disorder detected by *in vivo* ^{31}P and 7Li magnetic resonance spectroscopy, *J Affect Disord* **27**(1) (1993), 53–59.
[133] T. Kato, T. Shioiri and J. Murashita, et al., Lateralized abnormality of high energy phosphate metabolism in the frontal lobes of patients with bipolar disorder detected by phase-encoded ^{31}P-MRS, *Psychol Med* **25**(3) (1995), 557–566.
[134] T. Kato, T. Inubushi and N. Kato, Magnetic resonance spectroscopy in affective disorders, *J Neuropsychiatry Clin Neurosci* **10**(2) (1998), 133–147.
[135] O. Miatto, R.G. Gonzalez, F. Buonanno and J.H. Growdon, *In vitro* ^{31}P NMR spectroscopy detects altered phospholipid metabolism in Alzheimer's disease, *Can J Neurol Sci* **13**(4) (1998), 535–539.
[136] G.G. Brown, S.R. Levine and J.M. Gorell, et al., *In vivo* ^{31}P NMR profiles of Alzheimer's disease and multiple subcortical infarct dementia, *Neurology* **39**(11) (1989), 1423–1427.
[137] R.G. Gonzalez, A.R. Guimaraes, G.J. Moore, A. Crawley, L.A. Cupples and J.H. Growdon, Quantitative *in vivo* ^{31}P magnetic resonance spectroscopy of Alzheimer disease, *Alzheimer Dis Assoc Disord* **10**(1) (1996), 46–52.
[138] N.J. Minshew, G. Goldstein, S.M. Dombrowski, K. Panchalingam and J.W. Pettegrew, A preliminary ^{31}P MRS study of autism: evidence for undersynthesis and increased degradation of brain membranes, *Biol Psychiatry* **33**(11–12) (1993), 762–773.
[139] C.M. Moore, J.D. Christensen, B. Lafer, M. Fava and P.F. Renshaw, Lower levels of nucleoside triphosphate in the basal ganglia of depressed subjects: a phosphorous-31 magnetic resonance spectroscopy study, *Am J Psychiatry* **154**(1) (1997), 116–118.
[140] A.J. Richardson, I.J. Cox, J. Sargentoni and B.K. Puri, Abnormal cerebral phospholipid metabolism in dyslexia indicated by phosphorus-31 magnetic resonance spectroscopy, *NMR Biomed* **10**(7) (!997), 309–314.
[141] T. Munakata, R.D. Griffiths, P.A. Martin, S.A. Jenkins, R. Shields and R.H. Edwards, An *in vivo* ^{31}P MRS study of patients with liver cirrhosis: progress towards a non-invasive assessment of disease severity, *NMR Biomed* **6**(2) (1993), 168–172.
[142] D.K. Menon, J. Sargentoni and S.D. Taylor-Robinson, et al., Effect of functional grade and etiology on *in vivo* hepatic phosphorus-31 magnetic resonance spectroscopy in cirrhosis: biochemical basis of spectral appearances, *Hepatology* **21**(2) (1995), 417–427.
[143] R. Jalan, J. Sargentoni and G.A. Coutts, et al., Hepatic phosphorus-31 magnetic resonance spectroscopy in primary biliary cirrhosis and its relation to prognostic models, *Gut* **39**(1) (1996), 141–146.
[144] S.D. Taylor-Robinson, J. Sargentoni and J.D. Bell, et al., *In vivo* and *in vitro* hepatic ^{31}P magnetic resonance spectroscopy and electron microscopy of the cirrhotic liver, *Liver* **17**(4) (1997), 198–209.
[145] K.K. Changani, R. Jalan and I.J. Cox, et al., Evidence for altered hepatic gluconeogenesis in patients with cirrhosis using *in vivo* 31-phosphorus magnetic resonance spectroscopy, *Gut* **49**(4) (2001), 557–564.
[146] M. Matoba, H. Tonami, H. Yokota, K. Higashi and I. Yamamoto, [Assessment of functional severity on *in vivo* hepatic ^{31}P-MRS in diffuse hepatic disease: comparative studies with 99mTc-GSA], *Nippon Igaku Hoshasen Gakkai Zasshi* **60**(8) (2000), 439–444.
[147] P.W. Angus, R.M. Dixon and B. Rajagopalan, et al., A study of patients with alcoholic liver disease by ^{31}P nuclear magnetic resonance spectroscopy, *Clin Sci* (*Lond*) **78**(1) (1990), 33–38.
[148] D.K. Menon, M. Harris, J. Sargentoni, S.D. Taylor-Robinson, I.J. Cox and M.Y. Morgan, *In vivo* hepatic ^{31}P magnetic resonance spectroscopy in chronic alcohol abusers, *Gastroenterology* **108**(3) (1995), 776–788.
[149] M.R. Estilaei, G.B. Matson, G.S. Payne, M.O. Leach, G. Fein and D.J. Meyerhoff, Effects of chronic alcohol consumption on the broad phospholipid signal in human brain: an *in vivo* ^{31}P MRS study, *Alcohol Clin Exp Res* **25**(1) (2001), 89–97.

[150] M.R. Estilaei, G.B. Matson, G.S. Payne, M.O. Leach, G. Fein and D.J. Meyerhoff, Effects of abstinence from alcohol on the broad phospholipid signal in human brain: an *in vivo* ^{31}P magnetic resonance spectroscopy study, *Alcohol Clin Exp Res* **25**(8) (2001), 1213–1220.

[151] Y. Yamane, M. Umeda, T. O'Uchi, T. Mitsushima, K. Nakata and S. Nagataki, Phosphorus-31 nuclear magnetic resonance *in vivo* spectroscopy of human liver during hepatitis A virus infection, *Dig Dis Sci* **39**(1) (1994), 33–38.

[152] K. Kiyono, A. Shibata and S. Sone, et al., Relationship of ^{31}P MR spectroscopy to the histopathological grading of chronic hepatitis and response to therapy, *Acta Radiol* **39**(3) (1998), 309–314.

[153] C. Boesch, C. Elsing, H. Wegmuller, J. Felblinger, P. Vock and J. Reichen, Effect of ethanol and fructose on liver metabolism: a dynamic ^{31}Phosphorus magnetic resonance spectroscopy study in normal volunteers, *Magn Reson Imaging* **15**(9) (1997), 1067–1077.

[154] R. Smith, R.J. Newman, G.K. Radda, M. Stokes and A. Young, Hypophosphataemic osteomalacia and myopathy: studies with nuclear magnetic resonance spectroscopy, *Clin Sci* (*Lond*) **67**(5) (1984), 505–509.

[155] C.E. Brown, J.H. Battocletti, R. Srinivasan, J. Moore and P. Sigmann, *In vivo* ^{31}P NMR spectroscopy for evaluation of osteoporosis, *Lancet* **2**(8549) (1987), 37–38.

[156] J.P. Mattei, S. Confort-Gouny, J. Vion-Dury, H. Roux, J.P. Bisset and P.J. Cozzone, Study of bone mineralization using phosphorus 31 nuclear magnetic resonance spectroscopy. Results in a population of women with osteoporosis, *Rev Rhum Engl Ed* **62**(2) (1995), 91–97.

[157] L. Sieverding, W.I. Jung and J. Breuer, et al., Proton-decoupled myocardial ^{31}P NMR spectroscopy reveals decreased PCr/Pi in patients with severe hypertrophic cardiomyopathy, *Am J Cardiol* **80**(3A) (1997), 34A–40A.

[158] S. Neubauer, T. Krahe and R. Schindler, et al., ^{31}P magnetic resonance spectroscopy in dilated cardiomyopathy and coronary artery disease. Altered cardiac high-energy phosphate metabolism in heart failure, *Circulation* **86**(6) (1992), 1810–1818.

[159] T. Yabe, K. Mitsunami, T. Inubushi and M. Kinoshita, Quantitative measurements of cardiac phosphorus metabolites in coronary artery disease by ^{31}P magnetic resonance spectroscopy, *Circulation* **92**(1) (1995), 15–23.

[160] F. Sardanelli, F. Zandrino, G. Molinari, S. Cordone, L. Delfino and F. Levrero, Magnetic resonance spectroscopy of ischemic heart disease, *Rays* **24**(1) (1999), 149–164.

[161] C.W. Lee, S.J. Park and S.W. Park, et al., ^{31}P nuclear magnetic resonance evidence of skeletal muscle metabolic abnormalities in mitral stenosis, *Am J Cardiol* **78**(5) (1996), 588–591.

[162] R. Lodi, B. Rajagopalan and A.M. Blamire, et al., Cardiac energetics are abnormal in Friedreich ataxia patients in the absence of cardiac dysfunction and hypertrophy: an *in vivo* ^{31}P magnetic resonance spectroscopy study, *Cardiovasc Res* **52**(1) (2001), 111–119.

[163] R. Lodi, P.E. Hart and B. Rajagopalan, et al., Antioxidant treatment improves *in vivo* cardiac and skeletal muscle bioenergetics in patients with Friedreich's ataxia, *Ann Neurol* **49**(5) (2001), 590–596.

[164] W. Heindel, H. Kugel, F. Wenzel, D. Stippel, R. Schmidt and K. Lackner, Localized ^{31}P MR spectroscopy of the transplanted human kidney in situ shows altered metabolism in rejection and acute tubular necrosis, *J Magn Reson Imaging* **7**(5) (1997), 858–864.

[165] H. Kugel, H.J. Wittsack, F. Wenzel, D. Stippel, W. Heindel and K. Lackner, Non-invasive determination of metabolite concentrations in human transplanted kidney *in vivo* by ^{31}P MR spectroscopy, *Acta Radiol* **41**(6) (2000), 634–641.

[166] A. Zemtsov, L. Dixon and G. Cameron, Human *in vivo* phosphorus 31 magnetic resonance spectroscopy of psoriasis. A noninvasive tool to monitor response to treatment and to study pathophysiology of the disease, *J Am Acad Dermatol* **30**(6) (1994), 959–965.

[167] P.F. Daly, R.C. Lyon, P.J. Faustino and J.S. Cohen, Phospholipid metabolism in cancer cells monitored by ^{31}P NMR spectroscopy, *J Biol Chem* **262**(31) (1987), 14875–14878.

[168] J.S. Cohen, Phospholipid and energy metabolism of cancer cells monitored by ^{31}P magnetic resonance spectroscopy: possible clinical significance, *Mayo Clin Proc* **63**(12) (1988), 1199–1207.

[169] P.F. Daly and J.S. Cohen, Magnetic resonance spectroscopy of tumors and potential *in vivo* clinical applications: a review, *Cancer Res* **49**(4) (1989), 770–779.

[170] W. Negendank, Studies of human tumors by MRS: a review, *NMR Biomed* **5**(5) (1992), 303–324.

[171] M.O. Leach, Magnetic resonance spectroscopy applied to clinical oncology, *Technol Health Care* **2**(4) (1994), 235–246.

[172] L.N. Sutton, R.E. Lenkinski, B.H. Cohen, R.J. Packer and R.A. Zimmerman, Localized ^{31}P magnetic resonance spectroscopy of large pediatric brain tumors, *J Neurosurg* **72**(1) (1990), 65–70.

[173] S.R. Smith, P.A. Martin, J.M. Davies, R.H. Edwards and A.N. Stevens, The assessment of treatment response in non-Hodgkin's lymphoma by image guided ^{31}P magnetic resonance spectroscopy, *Br J Cancer* **61**(3) (1990), 485–490.

[174] R.M. Dixon, P.W. Angus, B. Rajagopalan and G.K. Radda, Abnormal phosphomonoester signals in ^{31}P MR spectra from patients with hepatic lymphoma. A possible marker of liver infiltration and response to chemotherapy, *Br J Cancer* **63**(6) (1991), 953–958.

[175] S.R. Smith, P.A. Martin and R.H. Edwards, Tumour pH and response to chemotherapy: an *in vivo* ^{31}P magnetic resonance spectroscopy study in non-Hodgkin's lymphoma, *Br J Radiol* **64**(766) (1991), 923–928.

[176] W.G. Negendank, K.A. Padavic-Shaller and C.W. Li, et al., Metabolic characterization of human non-Hodgkin's lymphomas *in vivo* with the use of proton-decoupled phosphorus magnetic resonance spectroscopy, *Cancer Res* **55**(15) (1955), 3286–3294.

[177] E.L. Mooyaart, R.L. Kamman and W.J. Boeve, *In vivo* ^{31}P nuclear magnetic resonance spectroscopy of osteosarcoma, *Cancer Treat Res* **62** (1993), 19–24.

[178] H.J. Hoekstra, W.J. Boeve, R.L. Kamman and E.L. Mooyaart, Clinical applicability of human *in vivo* localized phosphorus-31 magnetic resonance spectroscopy of bone and soft tissue tumors, *Ann Surg Oncol* **1**(6) (1994), 504–511.

[179] W.G. Negendank, MR spectroscopy of musculoskeletal soft-tissue tumors, *Magn Reson Imaging Clin N Am* **3**(4) (1995), 713–725.

[180] C.W. Li, A.C. Kuesel and K.A. Padavic-Shaller, et al., Metabolic characterization of human soft tissue sarcomas *in vivo* and *in vitro* using proton-decoupled phosphorus magnetic resonance spectroscopy, *Cancer Res* **56**(13) (1996), 2964–2972.

[181] E. Furman, R. Margalit, P. Bendel, A. Horowitz and H. Degani, *In vivo* studies by magnetic resonance imaging and spectroscopy of the response to tamoxifen of MCF7 human

breast cancer implanted in nude mice, *Cancer Commun* **3**(9) (1991), 287–297.

[182] T.E. Merchant, G.R. Thelissen, P.W. de Graaf, W. Den Otter and T. Glonek, Clinical magnetic resonance spectroscopy of human breast disease, *Invest Radiol* **26**(12) (1991), 1053–1059.

[183] T.A. Smith, J. Glaholm and M.O. Leach, et al., A comparison of *in vivo* and *in vitro* ^{31}P NMR spectra from human breast tumours: variations in phospholipid metabolism, *Br J Cancer* **63**(4) (1991), 514–516.

[184] C.J. Twelves, D.A. Porter and M. Lowry, et al., Phosphorus-31 metabolism of post-menopausal breast cancer studied *in vivo* by magnetic resonance spectroscopy, *Br J Cancer* **69**(6) (1994), 1151–1156.

[185] S.M. Ronen and M.O. Leach, Imaging biochemistry: applications to breast cancer, *Breast Cancer Res* **3**(1) (2001), 36–40.

[186] P.E. Kristjansen, M. Spang-Thomsen and B. Quistorff, Different energy metabolism in two human small cell lung cancer subpopulations examined by ^{31}P magnetic resonance spectroscopy and biochemical analysis *in vivo* and *in vitro*, *Cancer Res* **51**(19) (1991), 5160–5164.

[187] S. Leij-Halfwerk, P.C. Dagnelie, J.W. Van Den Berg, J.H. Wilson and P.E. Sijens, Hepatic sugar phosphate levels reflect gluconeogenesis in lung cancer: simultaneous turnover measurements and ^{31}P magnetic resonance spectroscopy *in vivo*, *Clin Sci* (*Lond*) **98**(2) (2000), 167–174.

[188] T.E. Merchant, L.T. van der Ven and B.D. Minsky, et al., ^{31}P NMR phospholipid characterization of intracranial tumors, *Brain Res* **649**(1–2) (1994), 1–6.

[189] P. Narayan, P. Jajodia and J. Kurhanewicz, et al., Characterization of prostate cancer, benign prostatic hyperplasia and normal prostates using transrectal 31phosphorus magnetic resonance spectroscopy: a preliminary report, *J Urol* **146**(1) (1991), 66–74.

[190] I.J. Cox, J.D. Bell and C.J. Peden, et al., *In vivo* and *in vitro* ^{31}P magnetic resonance spectroscopy of focal hepatic malignancies, *NMR Biomed* **5**(3) (1992), 114–120.

[191] I. Constantinidis, P.G. Braunschweiger and J.P. Wehrle, et al., ^{31}P-nuclear magnetic resonance studies of the effect of recombinant human interleukin 1 alpha on the bioenergetics of RIF-1 tumors, *Cancer Res* **49**(22) (1989), 6379–6382.

[192] M. Neeman and H. Degani, Early estrogen-induced metabolic changes and their inhibition by actinomycin D and cycloheximide in human breast cancer cells: ^{31}P and ^{13}C NMR studies, *Proc Natl Acad Sci USA* **86**(14) (1989), 5585–5589.

[193] R.G. Steen, Response of solid tumors to chemotherapy monitored by *in vivo* ^{31}P nuclear magnetic resonance spectroscopy: a review, *Cancer Res* **49**(15) (1989), 4075–4085.

[194] O.M. Redmond, E. Bell and J.P. Stack, et al., Tissue characterization and assessment of preoperative chemotherapeutic response in musculoskeletal tumors by *in vivo* ^{31}P magnetic resonance spectroscopy, *Magn Reson Med* **27**(2) (1992), 226–237.

[195] H.E. Moller, P. Vermathen and E. Rummeny, et al., *In vivo* ^{31}P NMR spectroscopy of human musculoskeletal tumors as a measure of response to chemotherapy, *NMR Biomed* **9**(8) (1996), 347–358.

[196] Z. Argov, N. De Stefano and D.L. Arnold, ADP recovery after a brief ischemic exercise in normal and diseased human muscle"a ^{31}P MRS study, *NMR Biomed* **9**(4) (1996), 165–172.

[197] A. Heerschap, C. Houtman, H.J. in 't Zandt, A.J. van den Bergh and B. Wieringa, Introduction to *in vivo* ^{31}P magnetic resonance spectroscopy of (human) skeletal muscle, *Proc Nutr Soc* **58**(4) (1999), 861–870.

[198] X. Ravalec, N. Le Tallec, F. Carre, J.D. de Certaines and E. Le Rumeur, Improvement of muscular oxidative capacity by training is associated with slight acidosis and ATP depletion in exercising muscles, *Muscle Nerve* **19**(3) (1996), 355–361.

[199] M.R. Smith, Non-Hodgkin's lymphoma, in:*Current Problems in Cancer,* (Vol. XX), S.D. Williams, R. Goulet and G. Thomas, eds, St. Louis, MO: Mosby, 1966.

[200] A predictive model for aggressive non-Hodgkin's lymphoma. The International Non-Hodgkin's Lymphoma Prognostic Factors Project, *N Engl J Med* **329**(14) (1993), 987–994.

[201] R. Ristamaki, H. Joensuu, K.O. Soderstrom and S. Jalkanen, CD44v6 expression in non-Hodgkin's lymphoma: an association with low histological grade and poor prognosis, *J Pathol* **176**(3) (1995), 259–267.

[202] P. Drillenburg, V.J. Wielenga and M.H. Kramer, et al., CD44 expression predicts disease outcome in localized large B cell lymphoma, *Leukemia* **13**(9) (1999), 1448–1455.

[203] H. Inagaki, S. Banno, A. Wakita, R. Ueda and T. Eimoto, Prognostic significance of CD44v6 in diffuse large B-cell lymphoma, *Mod Pathol* **12**(5) (1999), 546–552.

[204] P. Korkolopoulou, M.K. Angelopoulou and F. Kontopidou, et al., Prognostic implications of proliferating cell nuclear antigen (PCNA), AgNORs and p53 in non-Hodgkin's lymphomas, *Leuk Lymphoma* **30**(5–6) (1998), 625–636.

[205] M.B. Moller, A.M. Gerdes, K. Skjodt, L.S. Mortensen and N.T. Pedersen, Disrupted p53 function as predictor of treatment failure and poor prognosis in B- and T-cell non-Hodgkin's lymphoma, *Clin Cancer Res* **5**(5) (1999), 1085–1091.

[206] R. Stauder, W. Eisterer, J. Thaler and U. Gunthert, CD44 variant isoforms in non-Hodgkin's lymphoma: a new independent prognostic factor, *Blood* **85**(10) (1995), 2885–2899.

[207] A.A. Alizadeh, M.B. Eisen and R.E. Davis, et al., Distinct types of diffuse large B-cell lymphoma identified by gene expression profiling, *Nature* **403**(6769) (2000), 503–511.

[208] J.R. Griffiths, E. Cady, R.H. Edwards, V.R. McCready, D.R. Wilkie and E. Wiltshaw, ^{31}P-NMR studies of a human tumour in situ, *Lancet* **1**(8339) (1983), 1435–1436.

[209] J. Murphy-Boesch, R. Srinivasan, L. Carvajal and T.R. Brown, Two configurations of the four-ring birdcage coil for ^{1}H imaging and ^{1}H-decoupled ^{31}P spectroscopy of the human head, *J Magn Reson B* **103**(2) (1994), 103–114.

[210] F. Hirata, S. Toyoshima, J. Axelrod and M.J. Waxdal, Phospholipid methylation: a biochemical signal modulating lymphocyte mitogenesis, *Proc Natl Acad Sci USA* **77**(2) (1980), 862–865.

[211] Y. Niwa and S. Taniguchi, Phospholipid base exchange in human leukocyte membranes: quantitation and correlation with other phospholipid biosynthetic pathways, *Arch Biochem Biophys* **250**(2) (1986), 345–357.

[212] Z. Kiss, K.S. Crilly and W.H. Anderson, Carcinogens stimulate phosphorylation of ethanolamine derived from increased hydrolysis of phosphatidylethanolamine in C3H/101/2 fibroblasts, *FEBS Lett* **336**(1) (1993), 115–118.

[213] Z. Kiss, M. Tomono and W.B. Anderson, Phorbol ester selectively stimulates the phospholipase D-mediated hydrolysis of phosphatidylethanolamine in multidrug-resistant MCF-7 human breast carcinoma cells, *Biochem J* **302**(Pt 3) (1994), 649–654.

[214] H. Gillham and K.M. Brindle, ^{31}P NMR measurements of the effects of unsaturated fatty acids on cellular phospholipid metabolism, *Magn Reson Med* **35**(4) (1996), 481–488.

[215] R.M. Dixon and M. Tian, Phospholipid synthesis in the lymphomatous mouse liver studied by ^{31}P nuclear magnetic resonance spectroscopy *in vitro* and by administration of 14C-radiolabelled compounds *in vivo*, *Biochim Biophys Acta* **1181**(2) (1993), 111–121.

[216] C.P. Thomas, R.M. Dixon and M. Tian, et al., Phosphorus metabolism during growth of lymphoma in mouse liver: a comparison of ^{31}P magnetic resonance spectroscopy *in vivo* and *in vitro*, *Br J Cancer* **69**(4) (1994), 633–640.

[217] R.K. Sharma and V. Jain, Radiotherapeutic response of Ehrlich ascites tumor cells perfused in agarose gel threads and implanted in mice. A ^{31}P MR spectroscopy study, *Strahlenther Onkol* **177**(4) (2001), 212–219.

[218] J.D. Bell and K.K. Bhakoo, Metabolic changes underlying ^{31}P MR spectral alterations in human hepatic tumours, *NMR Biomed* **11**(7) (1998), 354–359.

[219] R. Dahiya, B. Boyle, H.D. Park, J. Kurhanewicz, J.M. Macdonald and P. Narayan, 13-cis-retinoic acid-mediated growth inhibition of DU-145 human prostate cancer cells, *Biochem Mol Biol Int* **32**(1) (1994), 1–12.

[220] R. Kalra, K.E. Wade and L. Hands, et al., Phosphomonoester is associated with proliferation in human breast cancer: a ^{31}P MRS study, *Br J Cancer* **67**(5) (1993), 1145–1153.

[221] G.M. Glazer, S.R. Smith, T.L. Chenevert, P.A. Martin, A.N. Stevens and R.H. Edwards, Image localized ^{31}P magnetic resonance spectroscopy of the human liver, *NMR Biomed* **1**(4) (1989), 184–189.

[222] S.F. Shedd, N.W. Lutz and W.E. Hull, The influence of medium formulation on phosphomonoester and UDP-hexose levels in cultured human colon tumor cells as observed by ^{31}P NMR spectroscopy, *NMR Biomed* **6**(4) (1993), 254–263.

[223] F. Podo, Tumour phospholipid metabolism, *NMR Biomed* **12**(7) (1999), 413–439.

[224] E.O. Aboagye and Z.M. Bhujwalla, Malignant transformation alters membrane choline phospholipid metabolism of human mammary epithelial cells, *Cancer Res* **59**(1) (1999), 80–84.

[225] R.M. Dixon, NMR studies of phospholipid metabolism in hepatic lymphoma, *NMR Biomed* **11**(7) (1998), 370–379.

[226] L. Bogin, M.Z. Papa, S. Polak-Charcon and H. Degani, TNF-induced modulations of phospholipid metabolism in human breast cancer cells, *Biochim Biophys Acta* **1392**(2–3) (1998), 217–232.

[227] Y.L. Ting, D. Sherr and H. Degani, Variations in energy and phospholipid metabolism in normal and cancer human mammary epithelial cells, *Anticancer Res* **16**(3B) (1996), 1381–1388.

[228] P.C. Dagnelie, J.D. Bell, S.C. Williams, T.E. Bates, P.D. Abel and C.S. Foster, Altered phosphorylation status, phospholipid metabolism and gluconeogenesis in the host liver of rats with prostate cancer: a ^{31}P magnetic resonance spectroscopy study, *Br J Cancer* **67**(6) (1993), 1303–1309.

[229] J. Lloveras, M. Hamza, H. Chap and L. Douste-Blazy, Action of hemicholinium-3 on phospholipid metabolism in Krebs II ascites cells, *Biochem Pharmacol* **34**(22) (1985), 3987–3993.

[230] A.C. Kuesel, G. Graschew, W.E. Hull, W. Lorenz and H.W. Thielmann, ^{31}P NMR studies of cultured human tumor cells. Influence of pH on phospholipid metabolite levels and the detection of cytidine 5'-diphosphate choline, *NMR Biomed* **3**(2) (1990), 78–89.

[231] W. Negendank, C.W. Li, K. Padavic-Shaller, J. Murphy-Boesch and T.R. Brown, Phospholipid metabolites in ^{1}H-decoupled ^{31}P MRS *in vivo* in human cancer: implications for experimental models and clinical studies, *Anticancer Res* **16**(3B) (1996), 1539–1544.

[232] J.L. Evelhoch, R.J. Gillies and G.S. Karczmar, et al., Applications of magnetic resonance in model systems: cancer therapeutics, *Neoplasia* **2**(1–2) (2000), 152–165.